Current Research in Pharmacology and Drug Discovery 3 (2022) 100117

Contents lists available at ScienceDirect

Current Research in Pharmacology and Drug Discovery

journal homepage: www.journals.elsevier.com/current-research-in-pharmacology-and-drug-discovery

Jagged-1 is induced by mTOR inhibitors in renal cancer cells through an Akt/ALK5/Smad4-dependent mechanism

David Danielpour [a,b,c,*], Sarah Corum [a], Patrick Leahy [a], Anusha Bangalore [a]

[a] Case Comprehensive Cancer Center Research Laboratories, The Division of General Medical Sciences-Oncology Case Western Reserve University, Cleveland, OH, 44106, USA
[b] Department of Pharmacology Case Western Reserve University, Cleveland, OH, 44106, USA
[c] Department of Urology University Hospitals of Cleveland, Cleveland, OH, 44106, USA

ARTICLE INFO

Keywords:
mTOR
Renal cancer
BEZ235
Rapamycin
EMT
KU-0063794
Akt
TGF-beta
Smad4
PI3K
Slug
Hic-5

ABSTRACT

The mammalian target of rapamycin (mTOR) plays an important role in the aggressiveness and therapeutic resistance of many cancers. Targeting mTOR continues to be under clinical investigation for cancer therapy. Despite the notable clinical success of mTOR inhibitors in extending the overall survival of patients with certain malignancies including metastatic renal cell carcinomas (RCCs), the overall impact of mTOR inhibitors on cancers has been generally disappointing and attributed to various compensatory responses. Here we provide the first report that expression of the Notch ligand Jagged-1 (JAG1), which is associated with aggressiveness of RCCs, is induced by several inhibitors of mTOR (rapamycin (Rap), BEZ235, KU-0063794) in human clear cell RCC (ccRCC) cells. Using both molecular and chemical inhibitors of PI3K, Akt, and TGF-β signaling, we provide evidence that the induction of JAG1 expression by mTOR inhibitors in ccRCC cells depends on the activation of Akt and occurs through an ALK5 kinase/Smad4-dependent mechanism. Furthermore, we show that mTOR inhibitors activate Notch1 and induce the expression of drivers of epithelial-mesenchymal transition, notably Hic-5 and Slug. Silencing JAG1 with selective shRNAs blocked the ability of KU-0063794 and Rap to induce Hic-5 in ccRCC cells. Moreover, Rap enhanced TGF-β-induced expression of Hic-5 and Slug, both of which were repressed in JAG1-silenced ccRCC cells. Silencing JAG1 selectively decreased the motility of ccRCC cells treated with Rap or TGF-β1. Moreover, inhibition of Notch signaling with γ-secretase inhibitors enhanced or permitted mTOR inhibitors to suppress the motility of ccRCC cells. We suggest targeting JAG1 may enhance therapeutic responses to mTOR inhibitors in ccRCCs.

1. Introduction

Renal cell carcinoma (RCC) is among the 10 most prevalent malignancies in the USA, with a projected annual incidence and mortality of 73,750 and 14,830 cases, respectively (Pandey and Syed, 2021). Approximately 70% of RCCs belong to a distinct subgroup of clear cell RCC (ccRCC), the majority of which are sporadic and occur as a single unilateral lesion. About one-third of patients with RCCs have distant metastases upon first diagnosis, with a 5-year survival of ≤20% (Kalra et al., 2016). Functional loss of the Von Hippel-Landau (VHL) tumor suppressor gene is the most common driver of ccRCC (Taylor et al., 2012). The VHL protein (pVHL) is a key component of the E3 ubiquitin ligase complex in charge of proteasome-mediated degradation of the transcription factors hypoxia-inducible factor (HIF)-1α and -2α following their hydroxylation by oxygen-dependent prolyl hydroxylase domain enzymes (PHDs). Thus, loss of pVHL in ccRCC leads to enhanced levels of

Abbreviations: ALK5, Activin-like kinase 5 (TGF-β type I receptor); ANOVA, Analysis of variance; BSA, Bovine serum albumin; ccRCC, Clear cell renal cell carcinoma; EDTA, Ethylenediaminetetraacetic acid; FBS, Fetal bovine serum; Hic-5, Hydrogen peroxide-inducible clone 5, also known as transforming growth factor beta induced transcript; IRS-1, Insulin receptor substrate-1; JAG1, Jagged-1; MAML-1, Mastermind-like protein-1; Myr, Myristoylated; mRCC, Metastatic renal cell carcinoma; mTORC1, Mammalian target of rapamycin complex 1; mTORC2, Mammalian target of rapamycin complex 2; PI3K, Phosphatidylinositol 3-kinase; Rap, Rapamycin; RCC, RCC; Rheb, Ras homologue enriched in brain; SE, Standard error; Slug, Snail family of transcription factors encoded by the SNAI2 gene; Smad, Mothers against decapentaplegic homolog; TβRI, Transforming growth factor β receptor type 1; TβRII, Transforming growth factor β receptor type 2; TGF-β, Transforming growth factor-beta; TSC, Tuberous Sclerosis Complex.

* Corresponding author. Wolstein Research Building, Room 3-532, 2103 Cornell Rd, Cleveland OH, 44106, USA.
E-mail address: dxd49@case.edu (D. Danielpour).

https://doi.org/10.1016/j.crphar.2022.100117
Received 10 January 2022; Received in revised form 20 June 2022; Accepted 30 June 2022

HIF-1α and HIF-2α, which bind to the hypoxia response elements (HRE) of the vascular endothelial growth factor (VEGF) genes to drive the overproduction of VEGF, leading to enhanced angiogenesis and thereby tumor growth (Kim et al., 2021a; Tirpe et al., 2019).

The major lines of therapeutics for newly diagnosed metastatic RCC (mRCC) (stage 4 disease) are tyrosine kinase inhibitors (TKIs) (i.e., sorafenib, sunitinib, pazopanib, and cabozantinib) targeting the VEGF receptors (VEGFRs), which block the heightened tumor angiogenesis associated with RCCs (Chowdhury and Drake, 2020). Immune therapy is also used in conjunction with TKIs. The rapamycin (Rap) analogs (rapalogs) everolimus (RAD-001) or temsirolimus (Torisel) have been shown in phase 2 and 3 clinical trials to moderately prolong the overall survival of patients with mRCC who fail VEGFR-selective TKI therapy (Staehler et al., 2021; Flaherty et al., 2015; Hess et al., 2009) and have thus gained enthusiastic support for their use as a part of a first or second-line therapy for mRCC (Pezzicoli et al., 2021; Cancel et al., 2021; Garcia and Danielpour, 2008).

The mammalian target of Rap (mTOR) is an attractive druggable target for the treatment of various malignancies, particularly since it is overactivated in cancers, and plays a focal role in the regulation of cell growth, survival, protein synthesis, and cellular metabolism (Saxton and Sabatini, 2017). Overactivation of mTORC1 in cancers is believed to occur predominantly through the phosphatidylinositol 3-kinase (PI3K)/Akt and mitogen-activated protein kinase (MAPK) pathways, which phosphorylate the Tuberous Sclerosis Complex (TSC2) and relieves TSC2's repression of the small G protein Ras homolog enriched in brain (Rheb), a direct activator of mTORC1 (Inoki et al., 2003). mTOR partners with several other proteins to form two functionally unique complexes known as mTOR complex 1 (mTORC1) and mTORC2. The enhanced activity of each of these complexes in cancer cells stimulates tumor growth, albeit through different mechanisms. mTORC1 can be distinguished from mTORC2 in several ways. Raptor is an obligate partner of mTORC1, while Rictor is an obligate partner of mTORC2. Rap robustly inhibits mTORC1 but not mTORC2, although prolonged exposure to Rap may also inhibit mTORC2 (Saxton and Sabatini, 2017; Sarbassov et al., 2004, 2006; Kim et al., 2002). Rap inhibits mTORC1 by first binding to FKBP12, which then interacts with and destabilizes mTORC1, thereby releasing Raptor from this complex (Drenan et al., 2004). In general, mTORC1 promotes tumor cell growth while mTORC2 drives tumor cell motility and invasiveness (Maru et al., 2013; Gupta et al., 2013; Smith et al., 2020).

Clinical use of rapalogs as single agents has had limited success in the therapy of most cancers, believed to be partly because of inefficient suppression of mTORC1, limited suppression of mTORC2, and compensatory feedback leading to activation of various survival pathways including PI3K, Akt, MAPK and Bcl-2 (Pezzicoli et al., 2021; Shi et al., 2005; Sun, 2021). The mTORC1 kinase operates in a negative-feedback loop to quell mitogenic activity in part through targeting insulin receptor substrate-1 (IRS-1) either directly (Shi et al., 2005; Tremblay and Marette, 2001; Easton et al., 2006) or indirectly through activation of Grb10, an inhibitor of IRS-1 and the insulin receptor (Hsu et al., 2011). Additionally, Rap promotes survival through activating autophagy by inhibiting mTORC1's phosphorylation and inhibition of the initiator of autophagy, ULK1 (Kim et al., 2011). Thus, inhibition of mTORC1 by Rap activates both cytostatic and cell survival responses. For these reasons, there has been great interest in the use of mTOR kinase inhibitors that inhibit both mTORC1 and mTORC2, and compounds that inhibit the kinase activity of both mTOR and PI3K (Alzahrani, 2019). Significant effort has been also focused on improving the clinical effectiveness of rapalogs by joint treatment with other cancer therapeutic drugs that intercept the compensatory responses of mTOR inhibitors. Such combination therapeutics have been found to synergize with mTOR inhibitors in promoting tumor cell death (Chauhan et al., 2016; Jacob et al., 2021).

Here we report a potential role of JAG1 in a compensatory response of ccRCC cells to mTOR inhibitors. Our discovery may shed new light on improving the effectiveness of rapalogs in the therapeutic management of mRCC.

2. Material and Methods

2.1. Materials

Sources were: DMEM/F12 (1:1, v/v) (Media Tech), characterized fetal bovine serum (FBS) (HyClone), BEZ235 and KU-0063794 (Selleck Chem); Rap, UO126, MK2206, ZSTK474 (LC labs), and recombinant human TGF-β1 (R&D Systems); LY294002, ALK5 inhibitor-II (ALK5i-II) 2-(3-(6-Methylpyridin-2-yl)-1H-pyrazol-4-yl)-1,5-naphthyridine), Compound E (EMD, Millipore); LY411575 (MedChemExpress); Thiazolyl Blue Tetrazolium Bromide (#M5655; Sigma-Aldrich); rabbit anti-Survivin IgG (#AF886) (R&D Systems), rabbit anti-Jagged-1 (#2620), rabbit anti-phospho-rS6 (S235/S236; #9205), rabbit anti-phospho-Akt1 (T308, #9655), rabbit anti-phospho-Akt1 (S473, #4060). rabbit anti-phospho-PRAS40 (T246, #2997), rabbit anti-Raptor (S792, #2083), rabbit anti-Slug (# 9585), rabbit anti-phospho-Smad2 (S245/S247; #3108), rabbit anti-phospho-rS6 (S235/S236; #2211S), rabbit anti-Notch1 (#4380), rabbit anti-Notch2 (#4530), rabbit anti-Notch3 (#5276), rabbit anti-Notch1 intracellular domain (NICD) (#4147), rabbit anti-IRS1 (S1101; #2385) (Cell Signaling Technology, Inc.); mouse anti-GAPDH (sc-51907), mouse anti-Smad4 (sc-7966), mouse anti-Akt1 (sc-5298) (Santa Cruz Biotechnologies, Inc.); mouse anti-β-Actin (#A-5441) (Sigma-Aldrich, Inc.); mouse anti-Hic-5 (#611165) (BD Transduction Laboratories).

2.2. Cell culture

The human HEK-293T and 786-O cell lines were acquired from American Type Culture Collection (ATCC), and RCC4 cells were purchased from Sigma-Aldrich. 786-O and RCC4 cells were cultured under antibiotic-free conditions in DMEM/Ham's F12 medium (1:1, v/v) with 5% FBS, as before (Danielpour et al., 2022). All cell lines were cultured in 5% CO_2 at 37 °C, passaged at subconfluent density, and were tested to be negative for mycoplasma by the MycoAlert® Kit from Lonza, Inc.

2.3. Affymetrix gene expression analysis

RCC4 cells were seeded at a density of 1.5×10^6 cells/10 ml/dishes in six 100-mm Falcon tissue culture dishes in DMEM/F12 (1:1, v/v) supplemented with 5% FBS. The next day, three dishes received a final concentration of 1 μM BEZ235 and the remaining three dishes received DMF vehicle control. Following 24 h treatment, cell monolayers were washed twice with cold phosphate-buffered saline (PBS) and total RNA from each dish was purified separately by RNeasy® (Qiagen). The purity of each RNA preparation was then confirmed by optimal A260/A280 ratios (~2.0; as measured by a NanoDrop UV spectrophotometer) and by UV inspection of the 28S and 18S RNA bands following electrophoresis on an agarose-MOPS gel (containing formaldehyde, and ethidium bromide). Then, 10 μg of total RNA from each preparation were pooled by the treatment group and delivered to the Case Western Reserve University Gene Expression and Genotyping Facility for further assessment of RNA integrity (using a Bioanalyzer 2100 (Agilent Technologies)) and gene expression analysis using Affymetrix GeneChip® Human Gene 1.0 ST Arrays. Affymetrix chips were filled with hybridization cocktails containing equal amounts of cDNA. After hybridization, the microarray chips were washed with identical wash protocols. Fluorescence intensities across all chips were normalized to the average overall signal intensity. Fluorescent signal intensities were quantified and individual sample gene expression data were exported as single numerical values in tab-delimited text files. Differences between means of each group were calculated and those that had fold changes of greater than or equal to 1.5 and whose differences were found to be statistically significant, using a one-tailed *t*-test, were sequestered into a list for submission to DAVID and gene set enrichment analysis.

2.4. Cell growth/viability assays

Crystal Violet Staining Assay: Cells trypsinized off subconfluent culture dishes were enumerated with a Countess™ Automated Cell Counter (Invitrogen, Inc.), plated with DMEM/F12 medium supplemented with 5% FBS in Falcon 12-well dishes at a density of 10,000 cells/1 ml/well and placed overnight in a Forma Scientific cell culture incubator (37 °C, 5% CO_2, 21% O_2). Cells were then treated with various agents, and after 4 days they were stained with crystal violet and quantified as previously described (Danielpour et al., 2019). The data, representing the average of triplicate determinations ± S.E., were plotted with GraphPad Prism.

MTT Assay: Cells trypsinized and enumerated as above were plated (with a Rainin multichannel electronic pipettor) in two separate Falcon 96-well dishes at a density of 1000 cells/90 μl/well with DMEM/F12 + 5% FBS and then placed overnight in a Forma Scientific cell culture incubator (37 °C, 5% CO_2, 21% O_2). Twelve wells from each dish contained only medium without cells as blank controls. Wells from one plate (designated day zero control) each received 10 μl of the above medium and 10 μl of MTT stock reagent (5 mg/ml Thiazolyl Blue Tetrazolium Bromide in phosphate-buffered saline) and were placed in the above incubator for 3 h. Wells from another dish were then treated with 10 μl of the above culture medium containing mTOR inhibitors or vehicle controls and returned to the incubator for an additional 72 h, after which each well was treated with 10 μl of MTT stock reagent as above. MTT reaction in each well was then blocked with 100 μl of MTT solubilization stock (10% SDS + 10 mM acetic acid) and dye solubilized overnight at 37 °C. Absorption at 570 nm was measured with a Tecan plate reader, subtracting values from the average of wells without cells. The data from 72 h treated cells, representing the average of 7 replicate determinations ± S.E., were plotted with GraphPad Prism following normalization to the day zero control readings.

2.5. Western blotting

RCC4 and 786-O cells (2×10^5 cells/2 ml DMEM/F12 + 5% FBS) were allowed 24 h for attachment to 6-well dishes (2 ml/well), and then treated as indicated. Following treatment, wells were washed twice with PBS, lysed with RIPA-EDTA buffer containing protease inhibitor cocktail, and clarified lysates were processed by Western blotting as described previously (Song et al., 2013). Samples were normalized to protein concentrations, as measured by a microtiter BCA protein assay using a bovine serum albumin (BSA) standard curve run in duplicate and a Tecan plate reader. Unknown samples were the average of triplicate determinations. For improving precision and efficiency, all pipetting manipulations were performed by Mettler Toledo/Rainin electronic pipettors in multi-dispense mode. Ponceau S staining of membranes was used to verify the uniformity of transfer.

2.6. Lentiviral-mediated silencing Smad4 and JAG1

Smad4 and JAG1 were silenced by RNA inteference with pLKO.1 lentiviral small hairpin RNA (shRNA) constructs (Smad4: TRCN0000010321, TRCN0000010322, TRCN0000010323; JAG1: TRCN0000244205, TRCN0000033443, TRCN0000033442) obtained from Sigma, Inc. Viral supernatants were produced by transfecting subconfluent monolayers of HEK-293T cells with pLKO.1 shRNAs, pMD2.G, and pCMV-dR8.74 as before (Song et al., 2013). pLKO.1 scrambled shRNA was used as a control. RCC4 and 786-O cells were transduced overnight with viral supernatant (MOI = 0.5) in the presence of 4 μg/ml protamine sulfate for 24 h, and 24 h after replacing with fresh growth medium, cells were treated with 2 μg/ml puromycin for several days or until all non-transduced cells died.

2.7. Adenoviral gene delivery of Akt and ALK5

Replication-incompetent adenoviral constructs for the expression of constitutively active and phosphorylation mutants of Akt1 and ALK5 were developed and packaged using an AdMax kit (Microbix Biosystems, Inc.) as described in a previous report from our group (Song et al., 2006).

2.8. Cell migration assays

Cell migration was measured by two approaches.

In the first approach, RCC cells were plated in 6-well dishes at a density of 4×10^5 cells/2 ml of DMEM/F12 containing 15 mM HEPES and 0.5% FBS and cultured overnight for attachment. Confluent cell monolayers were then wounded with a 200 μl micropipette tip, and wells were washed to remove the detached cells. Wound closure was assessed at various time intervals after wounding (0, 3 h, 6 h), using a Leica phase-contrast microscope with a camera attachment to capture digital images at a 4x objective.

In the second method, RCC cells were plated at a density of 2×10^4 cells/100 μl in 96-well ImageLock™ plates (Essen Bioscience), and after overnight for adhesion, monolayers were wounded with Woundmaker™ (Essen Bioscience), and floating cells were removed by washing wells twice using a custom-made 12-prong manifold aspirator and an Rainin 8 × 1000 μl multichannel electronic pipettor. Migration of cells in wounded monolayers (8 wells per treatment group) was monitored every 2 h by InCuyte Zoom Live-Cell Imaging (Essen Bioscience) and the kinetics of wound closure (expressed either as % Relative Wound Density, % Wound Closure, or μm Wound Width) was measured using the CellPlayer™ 96-well kinetic cell migration software (Essen Bioscience).

3. Results

3.1. mTOR inhibitors induce the expression of JAG1 in ccRCC cells

We explored the effectiveness of three mTOR inhibitors (Rap, KU-0063794, BEZ235) side-by-side at various doses in suppressing the growth of two ccRCC cell lines, RCC4 and 786-O, in cell culture. Rap selectively inhibits the activity of mTORC1, while KU-0063794 is a dual kinase inhibitor of mTORC1 and mTORC2 (Garcia-Martinez et al., 2009), and BEZ235 is a dual mTORC1/mTORC2 kinase inhibitor as well as a PI3K inhibitor (Maira et al., 2008). Cell growth was assessed after 4 days of treatment by crystal violet staining. Of these three inhibitors, Rap had the lowest specific activity, with a half-maximal inhibitory concentration (IC_{50}) of ~3.5 nM on each of these cell lines, while the IC_{50} of BEZ235 and KU-0063794 for both lines were 20 nM and 1 μM, respectively. Under these conditions, the maximum suppression of growth by Rap and BEZ235 was ~70% and ~90%, respectively (Fig. 1A and B).

Despite BEZ235's selectivity in inhibiting mTORC1, mTORC2, and PI3K, this drug has been shown to induce survival signals such as Akt activation and induced expression and activity of the androgen receptor in prostate cancer cells (Carver et al., 2011). Moreover, clinical use of BEZ235 on renal cancer was curtailed due to limited therapeutic response and dose-limiting toxicities (Carlo et al., 2016). The lack of objective response to BEZ235 in clinical trials suggests compensatory tumor-promoting feedback reactions by dual inhibition of mTOR and PI3K. To study the potential tumor survival pathways activated by combined suppression of mTOR and PI3K kinases in RCC cells, we used Affymetrix gene arrays to profile gene expression changes in RCC4 cells following 24 h treatment with 1 μM BEZ235, which is within the dose that suppresses both mTOR and PI3K kinases (Maira et al., 2008). Our analysis found that BEZ235 significantly altered the expression of 2100 genes by ≥ 1.5-fold. We submitted the BEZ235-induced gene changes to NCBI's Database for Annotation, Visualization, and Integrated Discovery (DAVID). Its algorithms employed a gene set enrichment analysis that

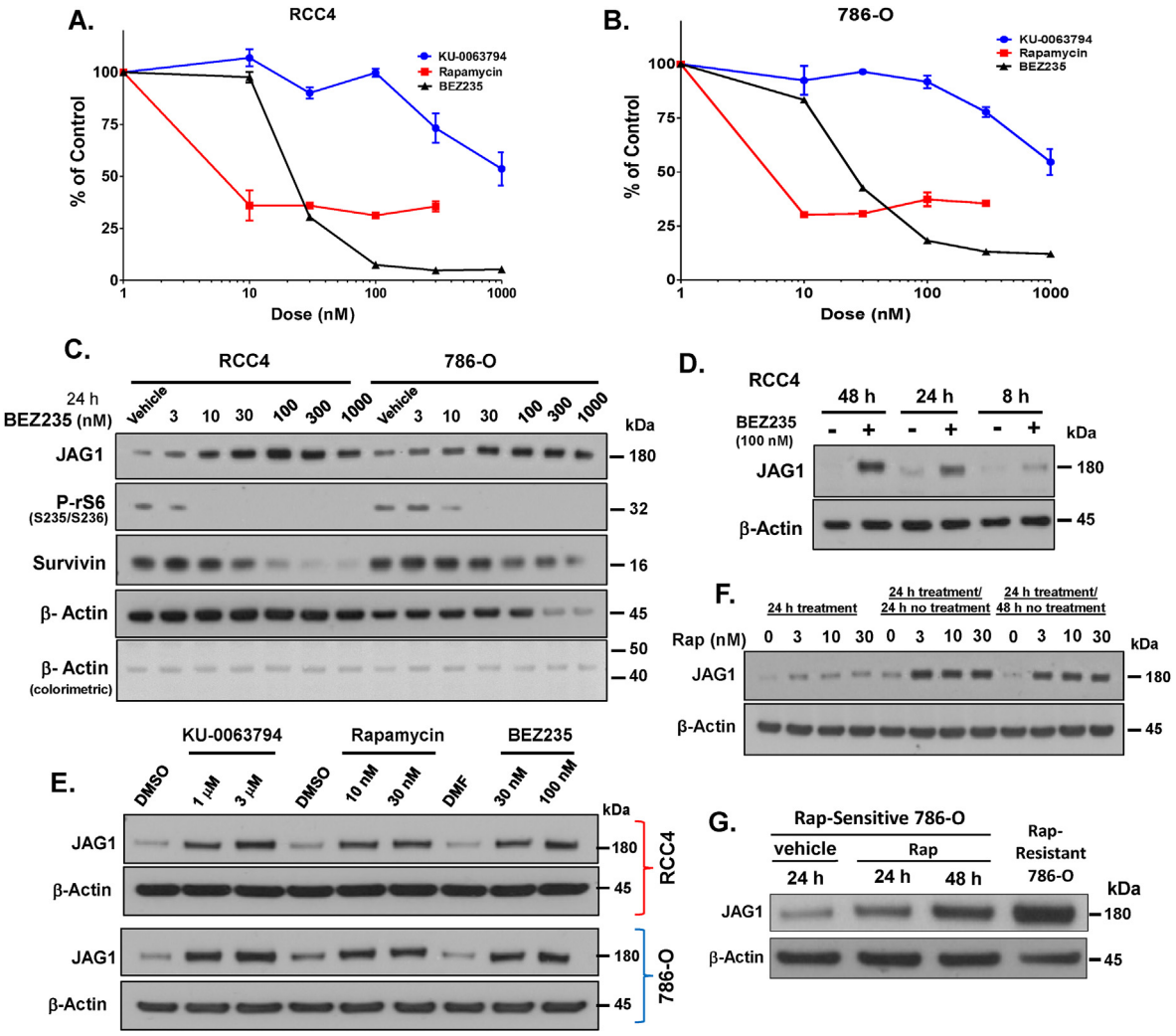

Fig. 1. mTOR inhibitors induce the expression of JAG1 in RCC cells. (A, B) Effect of various doses of Rap, KU-0063794, and BEZ235 on the growth of RCC4 **(A)** and 786-O **(B**) cells following four days of treatment was assessed by crystal violet staining, as described in "Materials and Methods". Optical densities from treated cells were expressed as the percent of vehicle-treated controls. Each data point represents the average of triplicate determinations (biological replicates) ± one standard error (SE) from the mean. **C)** Western blot analysis of the expression of JAG1, P-rS6$^{S356/S236}$, Survivin, and β-Actin on RCC4 and 786-O cells was assessed following 24 h of treatment with vehicle (DMF) and various doses of BEZ235. **D**) Induction of JAG1 following 8 h, 24 h, and 48 h of treating RCC4 cells with vehicle versus 100 nM BEZ235 was evaluated by Western blot. **E)** Comparison of the induced expression of JAG1 by 24 h of treating RCC4 and 786-O cells with growth inhibitory doses of KU-0063974, Rap, and BEZ235 was demonstrated by Western blot. (**F, G)** Western blot revealed that the induction of JAG1 by Rap in RCC4 cells is enhanced/retained 24 h and 48 h following removal of Rap **(F)** and JAG1 expression is elevated in a Rap-resistant 786-O variant generated by 45 days of continuous culturing with 100 nM Rap **(G)**. (For interpretation of the references to colour in this figure legend, the reader is referred to the Web version of this article.)

identified multiple survival and tumor-promoting pathways induced by BEZ235. This analysis revealed that BEZ235 alters the expression of many signaling pathways, such as Notch, EMT, TGF-β, Ras, MAPKs, and cell cycle in patterns that would be expected to promote tumor survival and aggressiveness (Supplementary Table 1). As JAG1 was one of the most highly induced tumor-promoting genes on our list, we studied the significance of this finding in RCC cells.

In a dose-response analysis, Western blots revealed that 10 nM BEZ235 robustly induced the expression of JAG1 in both RCC4 and 786-O cell lines, comparable to suppression of mTORC1 activity, as shown by the loss of the phosphorylation of ribosomal protein S6 (rS6) at S235/S236 (P–S6$^{S235/S236}$) (Fig. 1C), along with loss of Survivin, which is under the translational control of mTORC1 (Danielpour et al., 2019). However, 10 nM BEZ235 did not significantly suppress the growth of RCC4 or 786-O cells (Fig. 1A and B) or suppress the expression of Survivin (Fig. 1C), cyclin Ds and UBE2C (data not shown), consistent with compensatory mechanisms of growth control (such as induction of JAG1) of mTOR inhibition. At the IC_{50} required to inhibit cell growth, Rap and KU-0063794 comparably induced the expression of JAG1 in both cell lines by 24 h of treatment (Fig. 1E). The activity of BEZ235 in inducing JAG1 was seen as early as 8 h of treatment in RCC4 cells (Fig. 1D). In RCC4 cells, maximal induction of JAG1 by Rap at 24 h treatment occurred at 3 nM drug. JAG1 levels were further induced by 24 h–48 h even following the removal of Rap (Fig. 1F). Moreover, JAG1 was elevated in 786-O cells that were selected for Rap resistance following 45 days of continuous treatment/selection with Rap (Fig. 1G). These results support that JAG1 is a rapid and robustly induced protein following the therapeutic suppression of mTOR in human RCC.

3.2. Impact of PI3K, Akt, and MEK on the induction of JAG1 expression by mTOR inhibitors in RCC cells

We next investigated the potential roles of PI3K, Akt, and mitogen-activated protein kinase kinase (MEK) by which Rap induces the expression of JAG1 in RCC cells, using 20 nM Rap as a concentration that is within the safe zone for maximal induction of JAG1 expression by Rap.

For this, RCC4 cells were pretreated with either vehicle or optimally effective concentrations (based on published studies) of a PI3K inhibitor (LY294002,10 μM), an Akt kinase inhibitor (MK2206, 1 μM), or a MEK inhibitor (U0126, 10 μM) before a 24 h treatment with Rap. Interestingly, 10 μM LY294002 induced the expression of JAG1 to a level comparable to that induced by 20 nM of Rap, and when combined with 20 nM Rap, 10 μM LY294002 did not further induce the expression of JAG1 (Fig. 2A), suggesting that a common pathway is involved in the induction of JAG1 triggered by 20 nM Rap and by 10 μM LY294002. Pretreatment of RCC4 cells with U0126 (10 μM) induced JAG1 to a level comparable to that induced by 20 nM Rap; however, the joint treatment of Rap and U0126 further induced the expression of JAG1 in these cells, suggesting that Rap and U0126 induce JAG1 through different mechanisms. In contrast, inhibition of Akt by MK2206 at its effective inhibitory dose range entirely blocked the expression of JAG1 induced by Rap. Consistent with the literature, Rap induced phosphorylation of Akt (P-Akt^{T308}) (a direct target of PI3K) in RCC4 cells. As a confirmation of its activity as an Akt inhibitor on RCC4 cells, MK2206 inhibited P-Akt^{T308} as well as the subsequent phosphorylation of a direct target of Akt, PRAS40 (P-PRAS40^{T246}). LY294002 (10 μM) repressed Rap-induced phosphorylation of Akt1 and PRAS40. LY294002, MK2206, and U0126 similarly affected Rap-induced expression of JAG1 in the 786-O cells (Fig. 2B), suggesting common mechanisms of Rap-induced JAG1 expression in both cell lines. Treatment of RCC4 cells with 1 μM of ZSKT474, a more active and specific PI3K inhibitor than that of LY294002, similarly to 10 μM LY294002 induced the expression of JAG1 (Fig. 2A, C). Co-treatment of RCC4 cells with 1 μM ZSTK474 and Rap did not further induce JAG1 levels over that of the PI3K inhibitors or Rap alone, while 10 μM of ZSTK474 inhibited Rap-induced JAG1 (Fig. 2C). Although each of those PI3K inhibitors induced the expression of JAG1 at a concentration that inhibited PI3K activity, as seen by P-Akt1^{T308}, dose escalation of each of the PI3K inhibitors decreased rather than increased the levels of JAG1, suggesting a biphasic effect of PI3K in controlling JAG1 expression (Fig. 2C). The above results also suggest that robust inactivation of PI3K inhibits both basal and Rap-induced JAG1 expression.

In an MK2206 dose-response experiment, pre-treatment of RCC4 cells with 50 nM of MK2206 significantly suppressed the expression of Rap-induced JAG1 and levels of P-PRAS20^{T246}, and complete suppression by MK2206 occurred between 500 and 1000 nM (Fig. 2D). Similar to its ability to suppress JAG1 induced by Rap, MK2206 also suppressed the induction of JAG1 by KU-0063794, BEZ235, LY294002, and U0126 (Fig. 2E). These results suggest Akt may be critical for the induction of JAG1 by inhibitors of mTOR, PI3K, and MEK.

We next tested our hypothesis that Akt plays a role in the induction of JAG1 by mTOR inhibitors. In this effort, we employed a replication-incompetent adenoviral system to efficiently deliver a constitutively active form of Myc-tagged Akt1, myristoylated (Myr) Myc-Akt1 (Myr-Akt1) in RCC4 cells. The Myr residue (N-terminal fusion with src aa 1–11) anchors Akt1 to the plasma membrane independent of PI3K, enabling Akt1 to be phosphorylated at T308 by membrane-bound PDK-1 (Song et al., 2006; Downward, 1998; Kohn et al., 1996). Compared to the control Admax virus, transduction with the Myr-Akt1 overexpressing virus induced the expression of JAG1 to a level further than that induced by 20 nM Rap or 1 μM ZSTK474 (Fig. 2F). However, Rap but not ZSTK474 enhanced the expression of JAG1 by Myr-Akt1 (Fig. 2F). The level of JAG1 induction by Rap or Myr-Akt reflects the levels of P-Akt^{T308}, in contrast with that induced by ZSTK474, which suppressed P-Akt^{T308}.

In another set of experiments, we used three site-directed mutants of Myr-Akt1 (delivered by adenoviral transduction) to test the impact of the phosphorylation of Akt1 on the ability of Myr-Akt to induce the expression of JAG1 in RCC4 cells (Fig. 2G). Compared with wild-type Myr-Akt1, Myr-Akt1^{T308A} and Myr-Akt1^{S473A} less effectively induced expression of JAG1, and the double mutant Myr-Akt1$^{T308A/TS473A}$ did not induce JAG1 expression. Moreover, Myr-Akt1$^{T308A/TS473A}$ blocked JAG1 induction by Rap, consistent with a dominant-negative function of this mutant. These results suggest that phosphorylation of Akt1 at both T308 and S473 is required for the full activity of Akt1 in inducing the expression of JAG1 in RCC4 cells and that Rap-induced JAG1 expression in these cells requires activation of Akt1. Similar results were obtained in 786-O cells (Fig. 2H).

3.3. Role of the TGF-β type I receptor (ALK5) and Smad4 in the induction of JAG1 expression by mTOR inhibitors in RCC cells

Previous research in our laboratory supports that TGF-β signaling is activated in prostate epithelial cells following the suppression of mTOR (Song et al., 2006, 2013). Here we show that mTOR inhibitors also activate TGF-β signaling in RCC cells, as shown by enhanced levels of P-Smad2$^{S465/S467}$ (Fig. 3A). We, therefore, tested the role of TGF-β signaling in mTOR inhibitor-induced JAG1 expression using three approaches. In the first approach, we used a highly selective inhibitor of TGF-β signaling (ALK5i-II; chemical name 2-(3-(6-Methylpyridin-2-yl)-1H-pyrazol-4-yl)-1,5-naphthyridine) which inhibits autophosphorylation of ALK5 at $IC_{50} = 4$ nM in a kinase assay, without affecting the activity of related kinases such as the p38 MAPK (Gellibert et al., 2004). Treatment of RCC4 cells with 200 nM ALK5i-II completely blocked the expression of JAG1 by Rap without altering the phosphorylation of Akt or PRAS40 (Fig. 2A). In a dose-response experiment, suppression of Rap-induced JAG1 occurred at 25 nM ALK5i-II in these cells (Fig. 3B), which is within the dose of this drug's optimal effectiveness in selectively suppressing ALK5 kinase, suggesting that the effect of this inhibitor on blocking Rap-induced JAG1 is through antagonizing ALK5. In the next approach, we showed that adenoviral-mediated transduction of a kinase-dead ALK5 (ALK5^{T402A}), compared to control adenovirus, repressed both Rap-induced JAG1 and activation of Smad2 (P-Smad2$^{S465/S467}$) in RCC4 cells (Fig. 3C). On the other hand, adenoviral transduction of RCC4 cells with a constitutively active (CA) ALK5 (ALK5^{T402D}), which activated TGF-β signaling as shown by the phosphorylation of Smad2, enhanced the expression of JAG1 without altering the phosphorylation of Akt^{T308} (Fig. 3C). In the third approach, we blocked TGF-β signaling in RCC4 cells by shRNA-mediated silencing of Smad4, a co-Smad required for TGF-β responses (Zhou et al., 1998). Smad4 shRNAs or scrambled control shRNA were delivered to RCC4 cells by lentiviral transduction. Efficient silencing of Smad4 in these cells caused loss of Rap-induced JAG1 (Fig. 3D) or KU-0063794-induced JAG1 (Fig. 3E). Taken together, these results support that TGF-β signaling plays a pivotal role in the mechanism by which mTOR inhibitors induce the expression of JAG1.

We next assessed whether phosphorylation of Smad2 by Rap was mediated by activation of Akt. RCC4 cells were pre-treated for 2 h with vehicle or 1 μM MK2205 before 24 h of 20 nM Rap treatment. Levels of P-Smad2$^{S465/S467}$ induced by Rap were not significantly inhibited by MK2206 (Fig. 3F), suggesting that Rap activates TGF-β signaling in these cells independent of Akt activation.

3.4. mTOR inhibitors activate notch signaling in RCC cells

We next asked whether the induction of JAG1 by mTOR inhibitors activated JAG1 receptors in RCC cells. JAG1 is typically involved in paracrine signaling, anchored to adjacent cells bearing its receptors, Notch (Shen et al., 2021). Binding of JAG1 to full-length (FL) Notch activates Notch through enabling the cleavage of FL Notch at extracellular sites designated S2 and S3 by the metalloprotease ADAM10 and the γ-secretase complex, respectively (Shen et al., 2021). Cleavage at S2 first generates Notch transmembrane-intracellular domain (NTM), which is then cleaved at S3 to liberate Notch intracellular domain (NICD). NICD thereafter enters the nucleus where it transcriptionally induces the expression of Notch target genes (e.g., Hes and Hey families) by binding to the DNA binding protein CSL and allowing the recruitment of MAML-1 (Shen et al., 2021). Previous studies reported that Notch1 is expressed and functional in 786-O cells (Wu et al., 2016). Here we show that 786-O and RCC4 cells express FL and NTM of Notch1, Notch2, and Notch3 (Fig. 4A) and Notch1 NICD (Fig. 4C and D). However, 786-O cells express

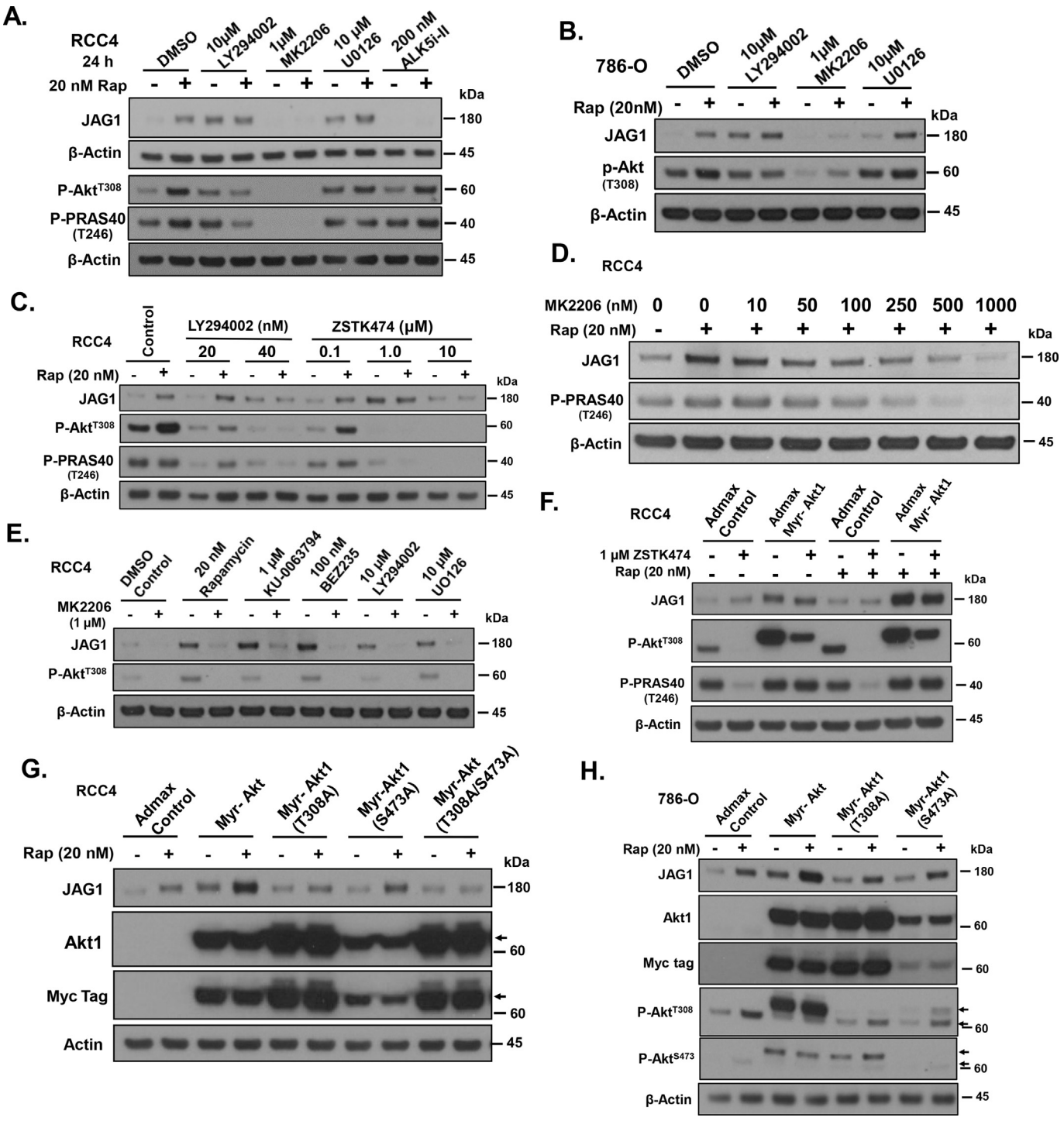

Fig. 2. The impact of PI3K, Akt, and MEK on the induction of JAG1 expression by mTOR inhibitors in RCC cells. A) RCC4 cells were pre-treated with either DMSO vehicle, LY294002 (10 μM), MK2206 (1 μM), U0126 (10 μM), or ALK5i-II (200 nM) for 2 h before 24 h of treatment with Rap (20 nM) followed by Western blotting for JAG1, and P-Akt1^{T308}, P-PRAS40^{T246}, and β-Actin. **B)** 786-O cells were pre-treated with either DMSO vehicle, LY294002 (10 μM), MK2206 (1 μM), and U0126 (10 μM) for 2 h before 24 h of treatment with Rap (20 nM) followed by Western blotting for JAG1, P-Akt1^{T308}, P-PRAS40^{T246}, and β-Actin. **C)** RCC4 cells were pre-treated with either DMSO vehicle, LY294002 (20 μM and 40 μM), or ZSTK474 (0.1, 1, 10 μM) for 2 h before 24 h of treatment with Rap (20 nM) and Western blotted as above. **D)** RCC4 cells were pretreated with various doses of MK2206 or vehicle (DMSO) 2 h before 24 h of treatment with 20 nM Rap followed by Western blotting for JAG1, P-PRAS40^{T246}, and β-Actin. **E)** RCC4 cells were treated either with DMSO vehicle or various doses of MK2206 (1–1000 nM) 2 h before 24 h treatment with 20 nM Rap followed by Western blotting for JAG1, P-PRAS40^{T246}, and β-Actin. **F)** RCC4 cells were infected with empty control AdMax or Myr-Akt1 expressing AdMax adenovirus 24 h before a 24-h treatment with either 1 μM ZSTK474 or 20 nM Rap followed by Western blotting for JAG1, P-Akt1^{T308}, and P-PRAS40^{T246}. **G, H)** RCC4 cells **(G)** or 786-O cells **(H)** were infected with AdMax adenoviral expressing constitutive active Akt (Myr-Akt1), Myr-Akt^{T308A}, Myr-Akt^{S473A}, Myr-Akt$^{T308A/S473A}$, or empty vector (AdMax control) for 24 h before a 24-h treatment with either 20 nM Rap or DMSO vehicle followed by Western blotting for JAG1, Akt, Myc-tag, P-Akt^{T308}, P-Akt^{S473}, and β-Actin, as shown in the respective blots.

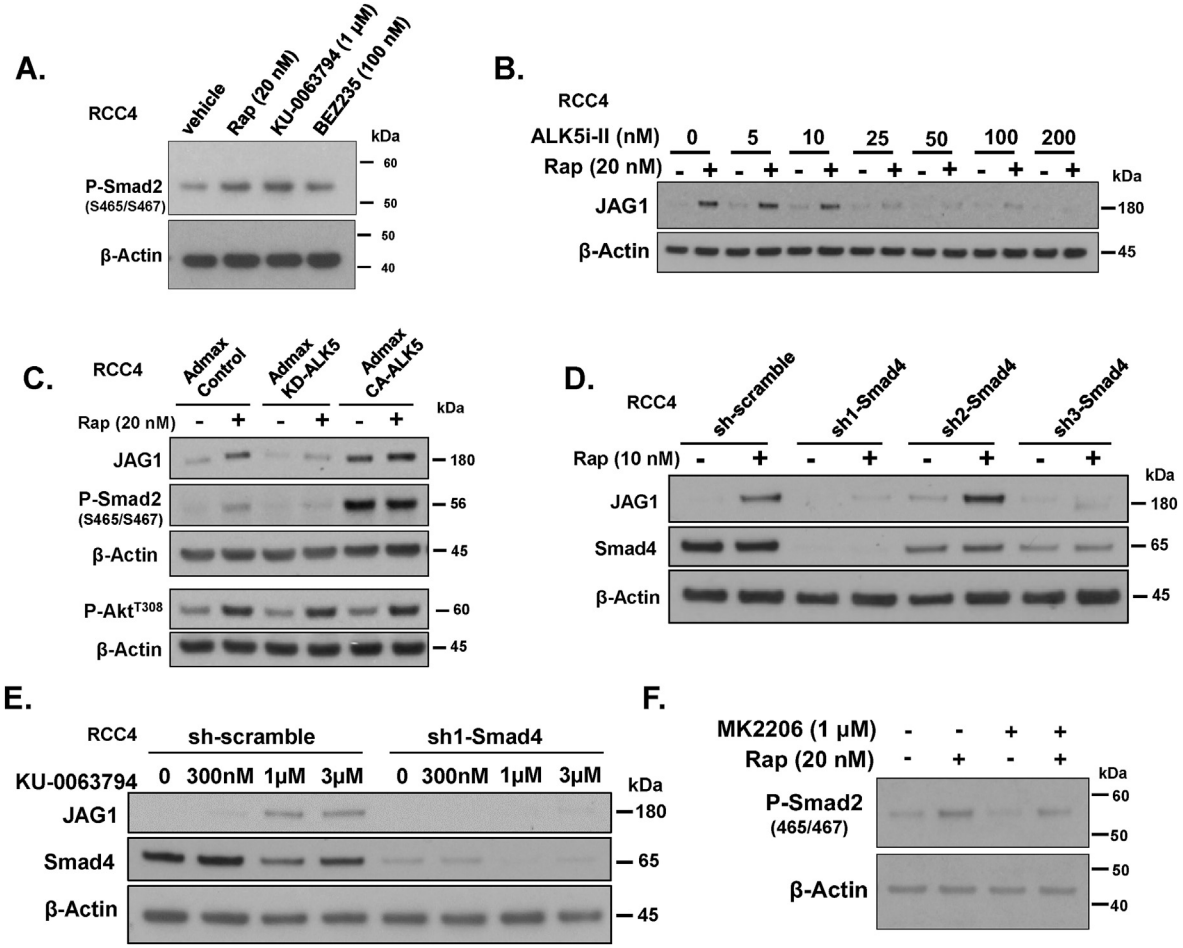

Fig. 3. Role of the TGF-β type I receptor (ALK5) and Smad4 in the induction of JAG1 expression by mTOR inhibitors in RCC cells. A) RCC4 cells were treated with 20 nM Rap, 1 μM KU-0063794, or 30 nM BEZ235 for 24 h, and then P-Smad2$^{S465/S467}$ and β-Actin were assessed by Western blot. **B)** RCC4 cells were treated with various doses of the TGF-β receptor type I inhibitor (ALK5i-II) or vehicle control 2 h before a 24 h treatment with DMSO vehicle or 20 nM Rap. Cell lysates were Western blotted for expression of JAG1 or β-Actin. **C)** RCC4 cells were infected for 24 h with empty Admax control, AdMax expressing kinase-dead (KD) ALK5 or constitutively active (CA) ALK5, followed by a 24 h treatment with vehicle control or 20 nM Rap, and cell lysates were assessed for expression of JAG1, P-Smad2$^{S465/S467}$, P-Akt^{T308}, and β-Actin. **D, E)** RCC4 cells were stably silenced for the expression of Smad4 by lentiviral transduction of three different shRNAs targeting Smad4 versus scrambled shRNA as described in "Materials and Methods" and then treated with vehicle or Rap **(D)** or vehicle and KU-0063794 **(E)**, followed by Western blotting for JAG1, Smad4, and β-Actin. **F)** RCC4 cells were pre-treated with vehicle or 1 μM MK2206 for 2 h before a 24 h of treatment with vehicle or 20 nM Rap, and P-Smad$^{S465/S467}$ was assessed by Western blot. All blots were reprobed for expression of β-Actin as a loading control.

higher levels of FL and NTM of Notch1 compared to RCC4 cells, whereas RCC4 express higher levels of Notch3 NTM compared to 786-O cells (Fig. 4A–D). Importantly, Rap, KU-0063794, and BEZ235 robustly elevate amounts of Notch1 NICD in 786-O cells (Fig. 4B and C) and Notch3 NTM in RCC4 cells (Fig. 4D). Although Rap, KU-0063794, and BEZ235 also cleaved Notch1 in RCC4 cells (Fig. 4D), under comparable conditions Western blot images of NICD were weak in RCC4 cells compared to 786-O cells. These results strongly support that mTOR inhibitors significantly activate Notch in RCC cells, consistent with the induced expression of JAG1.

3.5. Role of JAG1 in the induced expression of Slug and Hic-5 by mTOR inhibitors

Our microarray gene expression data on RCC4 cells revealed that BEZ235 induced the expression of the SNAI2 gene whose protein product is named Slug (Supplementary Table 1). Slug is transcriptionally induced by TGF-β and plays an important role in TGF-β-induced epithelial-mesenchymal transition (EMT) (Wirsik et al., 2021; Naber et al., 2013). Treatment of 786-O cells with KU-0063794, Rap, or BEZ235 for 1–3 days induced the expression of Slug and Hic-5 (Fig. 5B–D); Hic-5 is a TGF-β-induced protein involved in EMT (Pignatelli et al., 2012; Tumbarello and Turner, 2007). To test the role of JAG1 induction in mediating the expression of Slug and Hic-5, we silenced the expression of JAG1 with three shRNAs (sh1-JAG1, sh2-JAG1, sh3-JAG1) delivered by lentiviral transduction. At least two of those constructs efficiently silenced the expression of JAG1 (compared to scrambled shRNA control virus) induced by KU-0063794 (Fig. 5A). Silencing the expression of JAG1 suppressed KU-0063794-induced Hic-5 but not Slug in 786-O cells (Fig. 5B). In another experiment with 786-O cells, we showed that TGF-β1 induced the expression of JAG1 to levels comparable to that induced by Rap, and co-treatment of TGF-β with Rap induced the levels of JAG1 more than the summation of each treatment alone (Fig. 5C). Moreover, each treatment induced the expression of Slug and Hic-5 in a similar synergistic manner. Silencing JAG1 robustly suppressed the induction of Slug by TGF-β1 and suppressed the induction of Hic-5 by co-treatment with Rap and TGF-β1. Collectively, these results suggest that JAG1 plays an important role in the induced expression of 1) Hic-5 by KU-0063794, Rap, TGF-β1, or Rap + TGF-β1, and 2) Slug by TGF-β1 or by Rap + TGF-β1. Moreover, our data suggest that Rap and TGF-β1 work synergistically to promote EMT drivers (JAG1, Hic-5, and Slug).

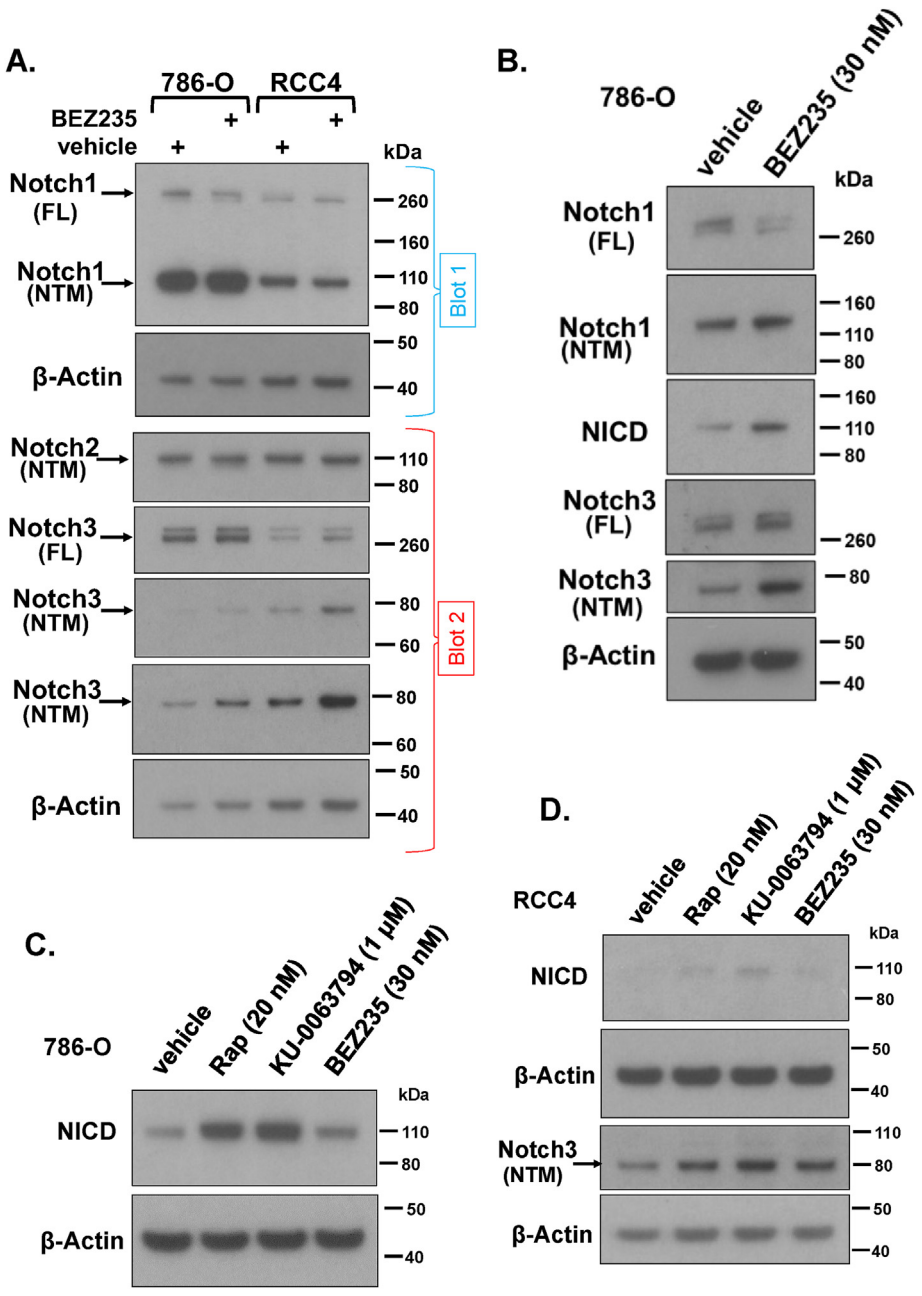

Fig. 4. Expression and activation of Notch in 786-O and RCC4 cells following treatment with mTOR inhibitors. A) Comparison of the relative levels of FL and NTM of Notch1, Notch2, and Notch3 in 786-O and RCC4 cells after 24 h of treatment with 30 nM BEZ235 or vehicle was assessed by Western blotting. **B)** Expression of FL, NTM, and NICD of Notch1 versus FL and NTM of Notch3 in 786-O cells treated for 24 h with 30 nM BEZ235 or vehicle was assessed by Western blotting. **C, D)** Effect of Rap, KU-0063794, and BEZ235 on the expression of Notch1 NICD or Notch3 NTM in 786-O **(C)** and RCC4 **(D)** cells was determined by Western blotting. All blots were reprobed for expression of β-Actin as a loading control.

3.6. The induced expression of JAG1 counteracts the effectiveness of mTOR inhibitors in suppressing cell migration

Notch signaling by JAG1 has been shown to drive tumor cell invasion, migration, and chemotherapy resistance by inducing EMT (Wang et al., 2009, 2017; Noseda et al., 2004). Zavadil and others (Zavadil et al., 2004) showed that TGF-β1 induced EMT in the mammary gland, kidney tubules, and epidermis and that such induction requires Smad3 and JAG1. We, therefore, studied the impact of Rap and TGF-β1 on the motility of 786-O cells using a standard wound-closure cell migration assay (Fig. 6A). To avoid the compounding effect of mTOR inhibitors on changes in cell growth, cell migration was assessed under low serum (0.5% FBS) growth medium that supports cell viability but not cell proliferation. Under this condition, neither TGF-β1 nor Rap alone altered the migration of 786-O cells (Fig. 6A). However, TGF-β1 and Rap each alone suppressed the migration of JAG1-silenced 786-O cells (Fig. 6A), suggesting that silencing JAG1 increased the effectiveness of TGF-β1 or Rap to suppress the motility of 786-O cells. We next used InCuyte ZOOM™ automated live-cell imaging to assess (at 2 h intervals) the impact of silencing JAG1 on the migration of 786-O cells treated with 30 nM Rap compared to vehicle control (Fig. 6B). Of note, data in Fig. 6B represent the average of 8 biological replicates ± S.E. and provide a kinetic analysis of cell migration (rate of change = slope of the curve). This experiment revealed that silencing JAG1 suppressed the migration of 786-O cells, in line with the function of JAG1 as an inducer of EMT. Although treatment with Rap compared to vehicle did not significantly suppress the migration of sh-scramble control 786-O cells, Rap significantly suppressed the migration of JAG1-silenced 786-O cells ($p < 0.01$). As illustrated in that graph, Rap depressed the slope of JAG1-silenced cells after 8 h, in line with the time needed for noticeable induction of JAG1 protein by Rap (Fig. 1D). Thus, our results here suggest that the induced expression of JAG1 by Rap antagonizes Rap's effect on suppressing the motility of RCC cells. Consistent with these results, MK2206, which blocked Rap-induced JAG1 (Fig. 2A, B, 2D), significantly enhanced the ability of Rap to

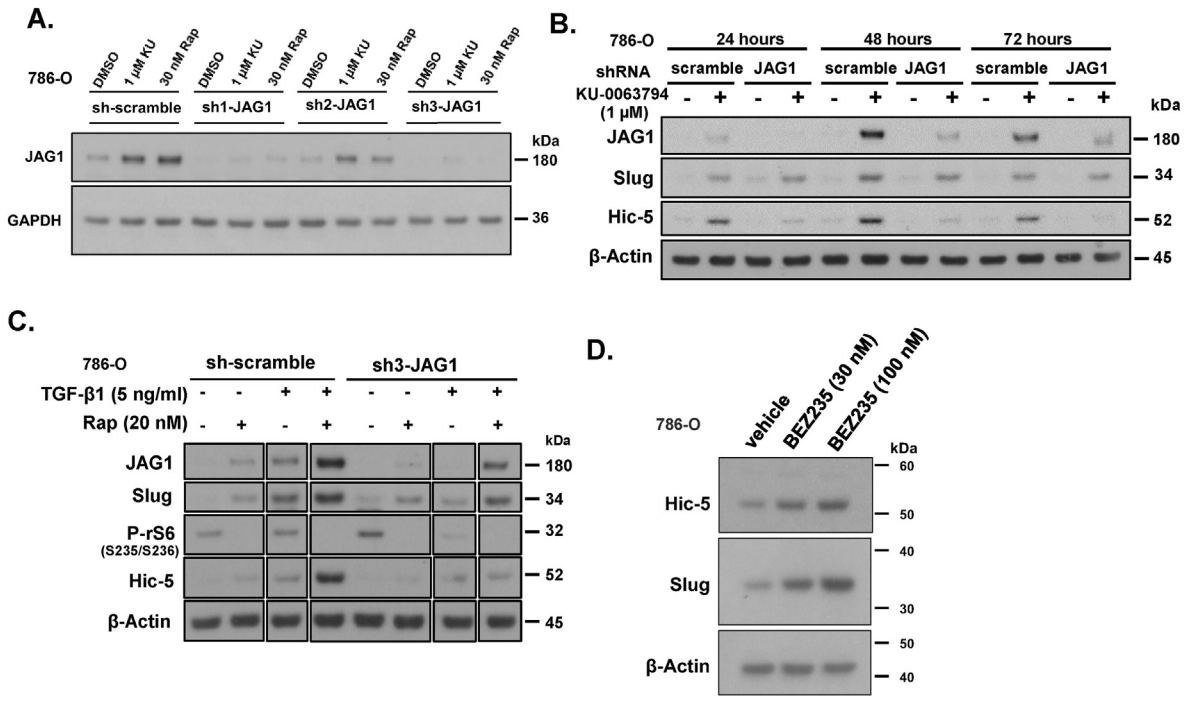

Fig. 5. Role of JAG1 in the induction of EMT markers by mTOR inhibitors and TGF-β1. 786-O cells were stably silenced for JAG1 by lentiviral transduction of three shRNAs targeting JAG1, and the expression of JAG1 was assessed following 24 h treatment with Rap, KU-0063794, or vehicle **(A)**. 786-O cells that were efficiently silenced for the expression of JAG1 by shRNAs versus shRNA scramble control cells were treated with either vehicle, KU-0063794 versus vehicle **(B)** or Rap (20 nM) ± TGF-β1 **(C)**, and cell lysates were Western blotted for JAG1, Slug, and Hic-5. 786-O cells were treated with vehicle or 30 nM–100 nM BEZ235 for 24 h and the expression of Slug and Hic-5 were assessed by Western blot **(D)**. All blots were reprobed for expression of β-Actin as a loading control.

suppress the motility of 786-O cells (Fig. 6C–E). As expected, MK2206 inhibited the migration of 786-O cells even without Rap.

We next tested the impact of JAG1 on the suppression of cell migration by other mTOR inhibitors. Similar to Rap, 30 nM BEZ235 did not significantly inhibit the migration of 786-O cells (Supplementary Fig. S1A). Our preliminary data indicate that pretreating 786-O cells for 8 h with 30 nM BEZ235 before wounding instead stimulated their motility compared to control (Supplementary Fig. S1B), consistent with a potential compensatory activity of this mTOR inhibitor. BEZ235 (100 nM), also did not significantly suppress the migration of sh-scramble 786-O cells. However, 100 nM BEZ235 significantly inhibited the migration of sh-JAG1 786-O cells after 10 h treatment (Fig. 7A). Similarly, treatment with 1 μM KU-0063794, significantly suppressed the migration of sh-scramble 786-O cells after 8 h treatment (Fig. 7B). However, 1 μM KU-0063794 more effectively inhibited the migration of sh-JAG1 786-O cells, particularly following 20–40 h of treatment (Fig. 7B–D). Here, wound closure was measured both by relative wound density and wound width. Two-way ANOVA analysis supported a significant interaction ($p < 0.001$) between the effect of sh-JAG1 and each mTOR inhibitor on suppression of cell migration (Fig. 7C and D). Side-by-side analysis with MTT cell viability/growth assay illustrated that mTOR inhibitors suppressed the fraction of viable 786-O cells equally in sh-scramble relative to sh-JAG1 transduced cells (Fig. 7E). The latter results suggest that JAG1 plays a role in repressing the inhibitory actions of mTOR inhibitors on RCC cell migration but not on their growth/survival.

We also silenced the expression of JAG1 in RCC4 cells with our shRNA constructs and found that silencing JAG1 in RCC4 cells robustly inhibited their growth and viability compared to shRNA scramble control (Supplementary Figs. S2A–B). Silencing JAG1 also changed the morphology of RCC4 cells and interfered with the formation of confluent cell monolayers compared to control cells when plated at the same high cell density. This made it difficult to accurately assess the impact of silencing JAG1 on the migration of RCC4 cells under comparable conditions, although our preliminary data (with cells brought to confluent density before wounding) support that silencing JAG1 robustly suppresses the migration of RCC4 cells and that the above mTOR inhibitors further suppress migration (Fig. 7F). Of note, 30 nM Rap and 30 nM BEZ235 each significantly suppressed the migration of the parental RCC4 cell line (without silencing JAG1), like that by 500 nM KU-0063794 (Supplementary Fig. S2C), indicating that mTOR inhibitors more effectively suppress the migration of RCC4 cells compared to 786-O cells.

Similar to the synergistic effect of MK2206 and Rap on suppressing cell motility, MK2206 enhanced the effectiveness of KU-0063794 and BEZ235 to suppress the migration of 786-O cells (Fig. 8A–C). Two-way ANOVA analysis of the above data demonstrated a statistically significant interaction between MK2206 and KU-0063794 ($p < 0.0001$) and between MK2206 and BEZ235 ($p < 0.01$) (Fig. 8B and C). Similarly, two-way ANOVA analysis indicated a synergistic interaction between MK2206 and KU-0063794 in inhibiting the migration of RCC4 cells (Fig. 8D). Moreover, MK2206 inhibited growth in both 786-O and RCC4 cells, and the combined effect of MK2206 and Rap or MK2206 and KU-0063794 was greater than the individual treatments alone (Fig. 8E and F).

3.7. γ-Secretase inhibitors permit mTOR inhibitors to inhibit the migration of RCC cells

We next used a different approach to test the role of Notch signaling on the effectiveness of mTOR inhibitors in suppressing the migration of RCC cells. This approach involved blocking JAG1 responses with highly potent γ-secretase inhibitors, LY411575 and Compound E. In a dose-response experiment, 10–100 nM LY411575 effectively suppressed Notch1 cleavage in 786-O cells (Fig. 9A). Similar to the impact of silencing JAG1, pretreatment with 100–1000 nM LY411575 enhanced the ability of Rap, KU-0063794, and BEZ235 to suppress the migration of 786-O cells (Fig. 9B–D). LY411575 (100 nM) also enhanced the effectiveness of BEZ235 to suppress cell migration of RCC4 cells (Fig. 9E). In all the above experiments with LY411575, this compound stimulated cell

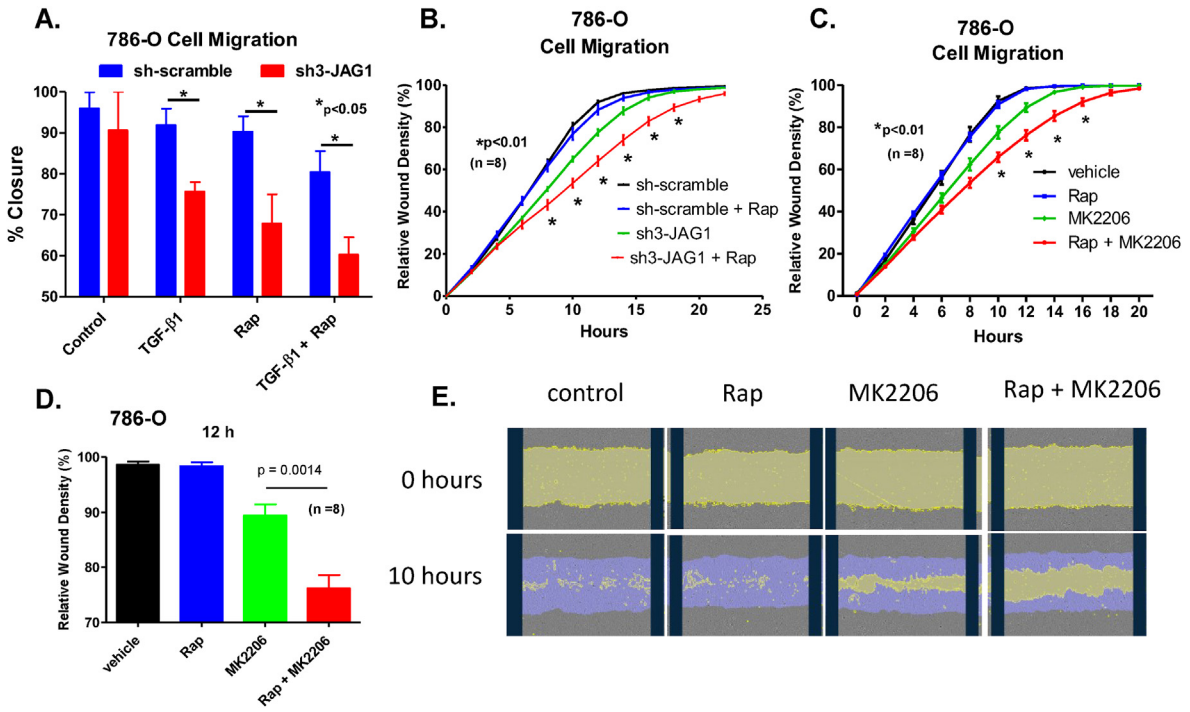

Fig. 6. The induced expression of JAG1 counteracts the effectiveness of Rap in suppressing the migration of 786-O cells. Scrambled control shRNA versus JAG1 shRNA-silenced 786-O cells, generated as discussed in the "Materials and Methods", were assessed for cell migration by a scratch wound assay following 24 h of treatment with vehicle or 10 nM Rap ±5 ng/ml TGF-β1 **(A)**, and kinetically (imaged at 2 h intervals and measured by Relative Wound Density) by InCucyte Zoom live-cell imaging between 0 and 24 h following treatment with 30 nM Rap or vehicle (**B**). **C)** Migration of 786-O cells (measured by Relative Wound Density) was assessed kinetically as in panel **B** following treatment with ±30 nM Rap ± 1 μM MK2206, using DMSO as vehicle control. **D)** Bar graph represents the 12 h time point of panel **C** analyzed for statistical significance (p-values) by two-way analysis of variance (ANOVA) using GraphPad Prism statistical tools. **E)** Representative phase-contrast images of wounded monolayers of 786-O cells captured at 0 h and 10 h following treatment with ±30 nM Rap ±1 μM MK2206. The yellow masks highlight wounds and the blue masks (at 10 h) highlight the closure of the original wound. (For interpretation of the references to colour in this figure legend, the reader is referred to the Web version of this article.)

migration at 100 nM or 1 μM in the absence of an mTOR inhibitor. However, when used alone, Compound E (100 nM) did not significantly suppress or enhance the migration of 786-O cells (Fig. 9F). Like LY411575, Compound E significantly enhanced the ability of Rap to inhibit wound closure. Moreover, Compound E did not significantly alter wound closure of control sh-scramble 786-O cells.

Our data thus support that silencing JAG1 enhances the action of mTOR inhibitors in suppressing the migration of RCC cells. How this translates into changes in their invasion through a matrix requires further work. Our preliminary study supports that silencing JAG1 enhances the invasiveness of 786-O cells through 25% Matrigel (Supplementation Figs. S3A and B). Although silencing JAG1 alone did not significantly alter the invasion of 786-O cells through this matrix, overexpression of JAG1 enhanced cell invasion (Supplementary Fig. S3C).

Taken together, these data support JAG1 and Notch as potential therapeutic targets for enhancing the effectiveness of rapalogs in patients with mRCC.

4. Discussion

Although there remains much enthusiasm for mTOR inhibitors in the treatment of mRCC, the limited understanding of the spectrum of compensatory mechanisms restrains their therapeutic potential (Sun, 2021). Here we provide the first demonstration that treatment of RCC cells with mTOR inhibitors induces the expression of the pro-metastatic protein JAG1, which is one of the key ligands for Notch signaling aberrantly elevated in various cancers including RCC where it is associated with poor overall survival (Wu et al., 2011; Sjolund et al., 2008). *In vitro* and *in vivo* studies demonstrate that Notch signaling is over-activated in RCC and suppression of Notch signaling with selective γ-secretase inhibitors suppresses RCC growth (Sjolund et al., 2008). Considering our data that mTOR inhibitors induce expression of JAG1 in RCC cells, it is likely that the induction of JAG1 intervenes in the full therapeutic effectiveness of mTOR inhibitors in RCC, and if so, suppressing such induction with a selective γ-secretase inhibitor may improve the clinical effectiveness of mTOR inhibitors in those cancers.

Our data in Fig. 2 suggest that mTOR inhibitors induce the expression of JAG1 through a mechanism that is dependent on the activation of Akt. We showed that activation of Akt1 signaling by expression of Myr-Akt1 alone significantly induces JAG1, enhances the ability of Rap to induce JAG1, and that P-Akt1$^{T308/S473}$ is necessary for the full ability of Akt1 to induce JAG1 expression (Fig. 2G and H). To the best of our knowledge, this is the first demonstration that Akt1 induces the expression of JAG1 in RCC cells. However, our results are consistent with a study that showed that conditional knockout of Akt1 in mouse endothelial cells markedly suppressed the expression of JAG1 along with inhibition of the Notch pathway in cardiac endothelial cells, causing the suppression of neovascularization and endothelial damage (Kerr et al., 2016). Consistent with this function, JAG1 cooperates with VEGFR to promote tumor angiogenesis (Oon et al., 2017), suggesting that JAG1 may mediate Akt1-induced angiogenesis and that high JAG1 levels may antagonize anti-VEGFR therapy. These findings support the use of an Akt inhibitor, such as MK2206, in enhancing the efficacy of both TKIs and rapalogs in the therapeutic management of mRCC. The mechanism by which Akt1 induces the expression of JAG1 remains unknown.

Our data (Fig. 2A–C) suggest that submaximal inhibition of PI3K with 10 μM LY294002 or 1.0 μM ZSTK474 induces basal levels of JAG1, while higher doses of these drugs dampen such induction. We speculate that this differential response may be PI3K isoform dependent, with certain PI3K isoforms (more sensitive to those drugs) suppressing basal levels of

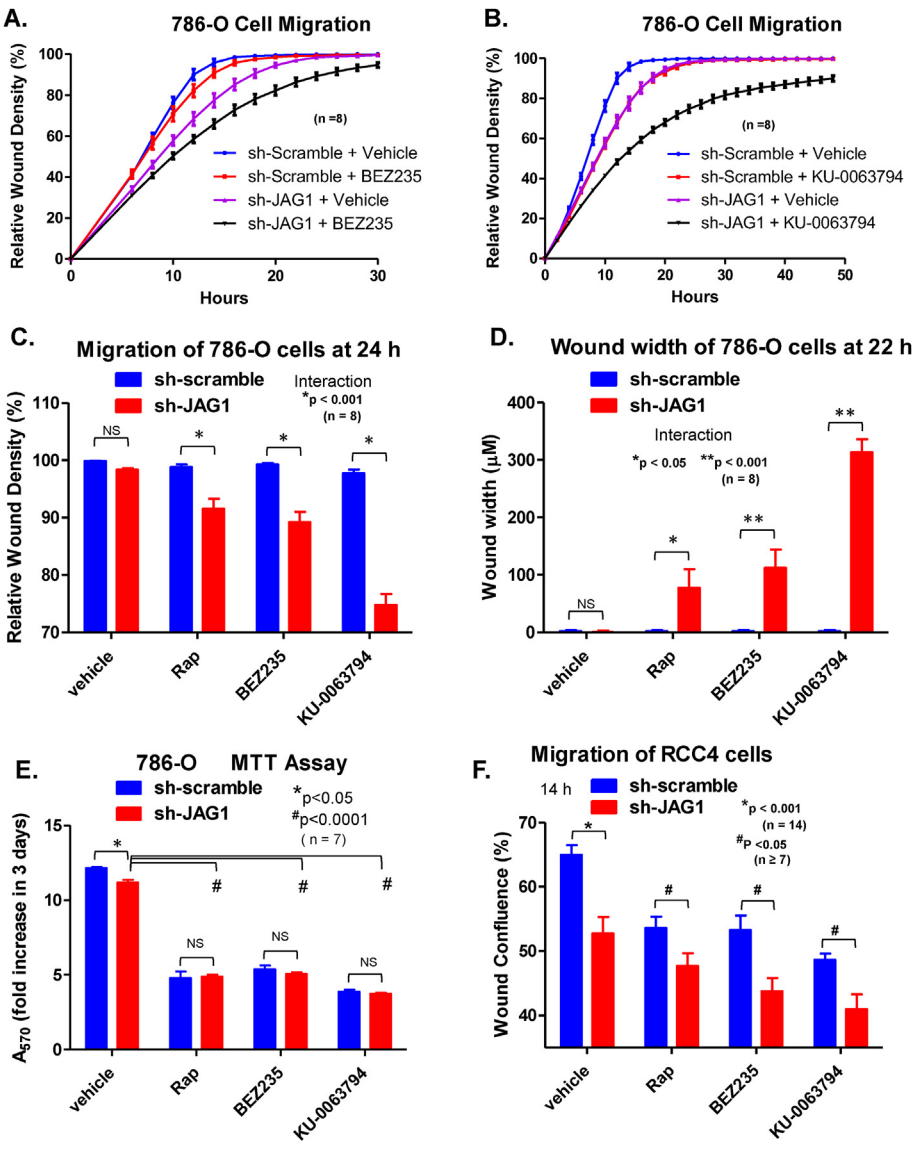

Fig. 7. Silencing JAG1 enhances the effectiveness of mTOR inhibitors on inhibiting the migration but not the growth of RCC cells. Scrambled control shRNA versus JAG1 shRNA-silenced 786-O cells, generated as discussed in the "Materials and Methods", were assessed for cell migration kinetically (imaged at 2 h intervals and measured by Relative Wound Density (%) by InCucyte Zoom live-cell imaging between 0 and 48 h following treatment with 100 nM BEZ235 compared to vehicle control **(A)** and 1 μM KU-0063794 compared to vehicle control **(B).** Comparative effects of 30 nM Rap, 100 nM BEZ235, and 1 μM KU-0063794 on the migration of JAG1 shRNA-silenced versus scramble control 786-O cells at 22 h and 24 h after wounding as measured by Relative Wound Density **(C)** and Wound Width **(D)**. **E)** Comparative effects of 30 nM Rap, 100 nM BEZ235, and 1 μM KU-0063794 on the viability/growth of JAG1 shRNA-silenced versus scramble shRNA control 786-O cells at 72 h after treatment as measured by an MTT assay described in Material and Methods. Data shown represent fold changes in A_{570} over day zero. **F)** Comparative effects of 30 nM Rap, 30 nM BEZ235, and 0.5 μM KU-0063794 on the migration of JAG1 shRNA-silenced versus scramble shRNA control RCC4 cells at 14 h after wounding measured by Wound Confluence (%). The data shown represent the average of 8 biological replicates **(A–D)** and ≥7 biological replicates **(E, F)** ± SE. Statistical significance and interactions were shown by two-way ANOVA using GraphPad Prism.

JAG1, whereas less drug-sensitive ones induce JAG1 expression. In line with the possibility of such isoform differential sensitivity, 10 μM LY294002 did not suppress basal levels of P-Akt^{T308} (Fig. 2A and B), while 40 μM LY294002 suppressed P-Akt^{T308} (Fig. 2C). Given the potential of such differential isoform sensitivity, it is likely that the compensatory effect of mTOR inhibitors on activation of PI3K is isoform-selective. Defining such a PI3K isoform-selective compensatory effect by mTOR inhibitors may have therapeutic value. Further work also beyond the scope of this study would be necessary to understand the mechanism by which suppression of MEK induces the expression of both JAG1 and P-Akt^{T308} (Fig. 2A, E), although our data suggest that such induction occurs through an Akt-dependent mechanism (Fig. 2E). Previous studies in HER2-positive breast cancer proposed that MEK inhibition activates Akt by relieving negative feedback on HER2 (Chen et al., 2017). Whether HER2 or another receptor tyrosine kinase is involved in the compensatory effect of MEK inhibition in renal cancer cells awaits further work.

Normal cells have important mechanisms that prevent the over-activation of mTORC1. In one such mechanism, S6K1 (which is directly activated by mTORC1) inactivates IRS-1 by phosphorylating IRS-1 at multiple serine residues (Shi et al., 2005; Tremblay and Marette, 2001; Easton et al., 2006; Zhang et al., 2008). One such residue is S1101. Thus, inhibition of mTORC1 can activate Akt indirectly by enabling IRS-1 to mediate PI3K activation by growth factor receptors. Our data (Supplementary Fig. S4) support this model, as we showed that mTORC1 inhibitors reduce levels of P-IRS-1^{S1101} in RCC cells.

Our data in Figs. 2A and 3A-F suggest that mTOR inhibitors induce the expression of JAG1 through a mechanism that is dependent on TGF-β signaling. As noted earlier, the induction of EMT by TGF-β in renal tubular epithelial cells was reported to be mediated by Smad3-dependent expression of JAG1 (Zavadil et al., 2004). Here we show that Smad4 is also involved in mTOR inhibitor-induced JAG1 expression, which our data suggests occurs through a TGF-β-dependent mechanism. It is thus likely that JAG1 functions in the aggressiveness of mRCC through a TGF-β-dependent mechanism requiring both Smads 3 and 4.

TGF-β1 is the founding member of the TGF-β superfamily of growth factors/cytokines that signal through binding to and activating transmembrane serine/threonine kinase receptors (Moses et al., 2016). There are three isoforms of TGF-β, namely TGF-β1, TGF-β2, and TGF-β3, each of which binds to the constitutively active kinase TGF-β type II receptor (TβRII) either directly or indirectly and causes TβRII to interact with and activate ALK5, which is the predominant TGF-β type I receptor (TβRI) that mediates TGF-β signaling (Massague, 1998). Upon activation, TβRI then activates Smads 2 and 3 by phosphorylating two serine residues in their C-termini. Once activated, Smads 2 and 3 enter the nucleus where

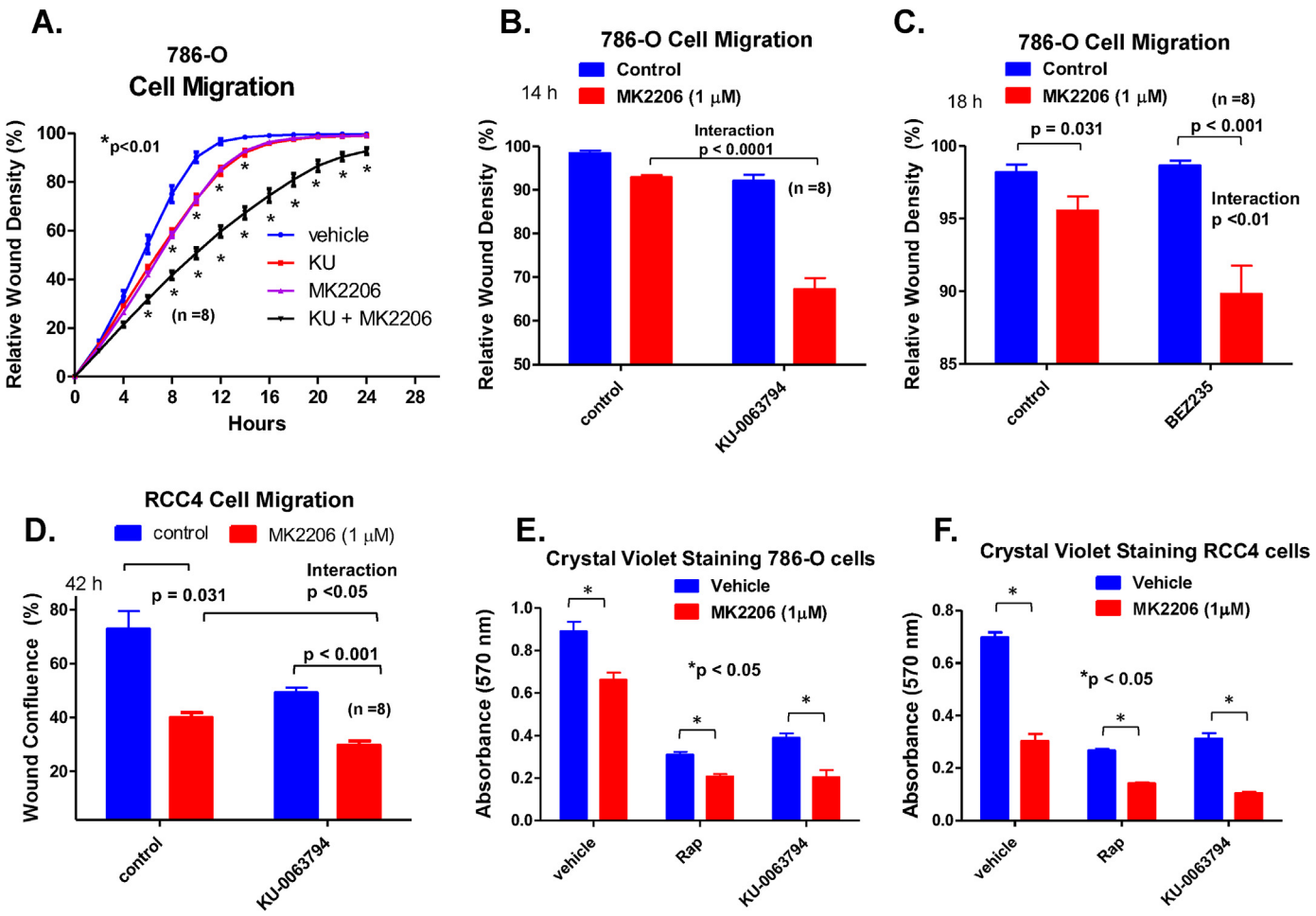

Fig. 8. MK2206 enhances the effectiveness of mTOR inhibitors in inhibiting the migration and growth of 786-O and RCC4 cells. A) Migration of 786-O cells (measured by Relative Wound Density) was assessed kinetically (as in Fig. 5B and C) following treatment with ±1 μM KU-0063794 ±1 μM MK2206, using DMSO as vehicle controls. **B)** Bar graph represents the 14 h time point of panel **A** analyzed by two-way ANOVA. **C)** Bar graph represents two-way ANOVA analysis at 18 h following treatment ±100 nM BEZ235 ±1 μM MK2206. **D)** Bar graph represents a two-way ANOVA analysis of RCC4 cell migration as measured by Wound Confluence (%) 42 h following treatment of ±1 μM KU0063794 ± 1 μM MK2206. Each point on the above graphs is the average of 8 biological replicates ± SE. P-values were calculated by two-way ANOVA using GraphPad Prism. **E, F)** Effect of 1 μM MK2206 on growth suppression of 786-O cells **(E)** and RCC4 cells **(F)** by 30 nM Rap and 1 μM KU-0063794 was assessed after four days of treatment by crystal violet staining, as described in "Materials and Methods". Each point on the graph is the average of 3 biological replicates ± SE. P-values were measured by ANOVA using GraphPad Prism statistical tools. (For interpretation of the references to colour in this figure legend, the reader is referred to the Web version of this article.)

they bind to Smad binding elements (SBEs), cooperatively with Smad4 and other transcriptional regulators, thereby controlling numerous cellular responses such as proliferation, apoptosis, cell migration, differentiation, development, and immunity (Jia and Meng, 2021). Given the functions of Smads as transcription factors, and that TGF-β induces the mRNA levels of JAG1 through a Smad3 and Smad4 dependent mechanism, we hypothesize that TGF-β drives the transcription of JAG1 by mTOR inhibitors (Fig. 10).

Although TGF-β functions as a tumor suppressor in numerous normal tissues and pre-neoplastic cells, TGF-β has tumor-promoting functions in neoplastic cells, particularly by driving EMT, tumor cell migration, invasion, metastasis, and immune evasion (Morikawa et al., 2016). Elevated expression of TGF-β1 and a TGF-β pathway signature are associated with aggressiveness of numerous cancers including ccRCC (Bao et al., 2021; Yang et al., 2010; Hao et al., 2019), and TGF-β1 is shown to promote migration, invasion, and bone metastasis of mRCC (Kominsky et al., 2007; Sitaram et al., 2016). Notch signaling has been reported to cooperate with TGF-β1 in driving the aggressiveness of ccRCC (Sjolund et al., 2011). Moreover, the elevation of HIF-1α levels in ccRCC enhances tumor invasiveness by TGF-β1 (Mallikarjuna et al., 2019). This is in line with the activation of TGF-β signaling in renal tubules by hypoxia (Kushida et al., 2016). Considering the above, loss of VHL function, which induces HIF-1α through a pseudo-hypoxia mechanism, may collaborate with TGF-β1 to enhance the aggressiveness of ccRCC.

Taken together, our data suggest that inhibition of mTOR induces the expression of JAG1 through a mechanism linked to the activation of both TGF-β and Akt signaling. Given the co-dependency of Akt and TGF-β on the induced expression of JAG1 by mTOR inhibitors, the role of Smads in the transcription of JAG1, and the kinase function of Akt, we speculate that Akt modulates a transcriptional co-regulator of JAG1 (Fig. 10). Further work will be necessary to test this hypothesis and identify such a co-regulator.

Our data in this report supporting that JAG1 is necessary for TGF-β to induce Slug and Hic-5 (Fig. 5) is consistent with previous reports that Notch and JAG1 are necessary for TGF-β-induced JAG1 and other genes associated with EMT in renal epithelial cells (Zavadil et al., 2004; Nyhan et al., 2010). Our study represents the first report that JAG1 is required for TGF-β-induced Hic-5 expression. The mechanism by which JAG1 promotes TGF-β-induced expression of Slug and Hic-5 is thus likely to involve Notch signaling (Fig. 6). Consistent with this hypothesis, Notch1 induces the expression of Hey1, which is a transcriptional regulator found to be associated with Smad3 in a Yeast-2 Hybrid screen (Colland

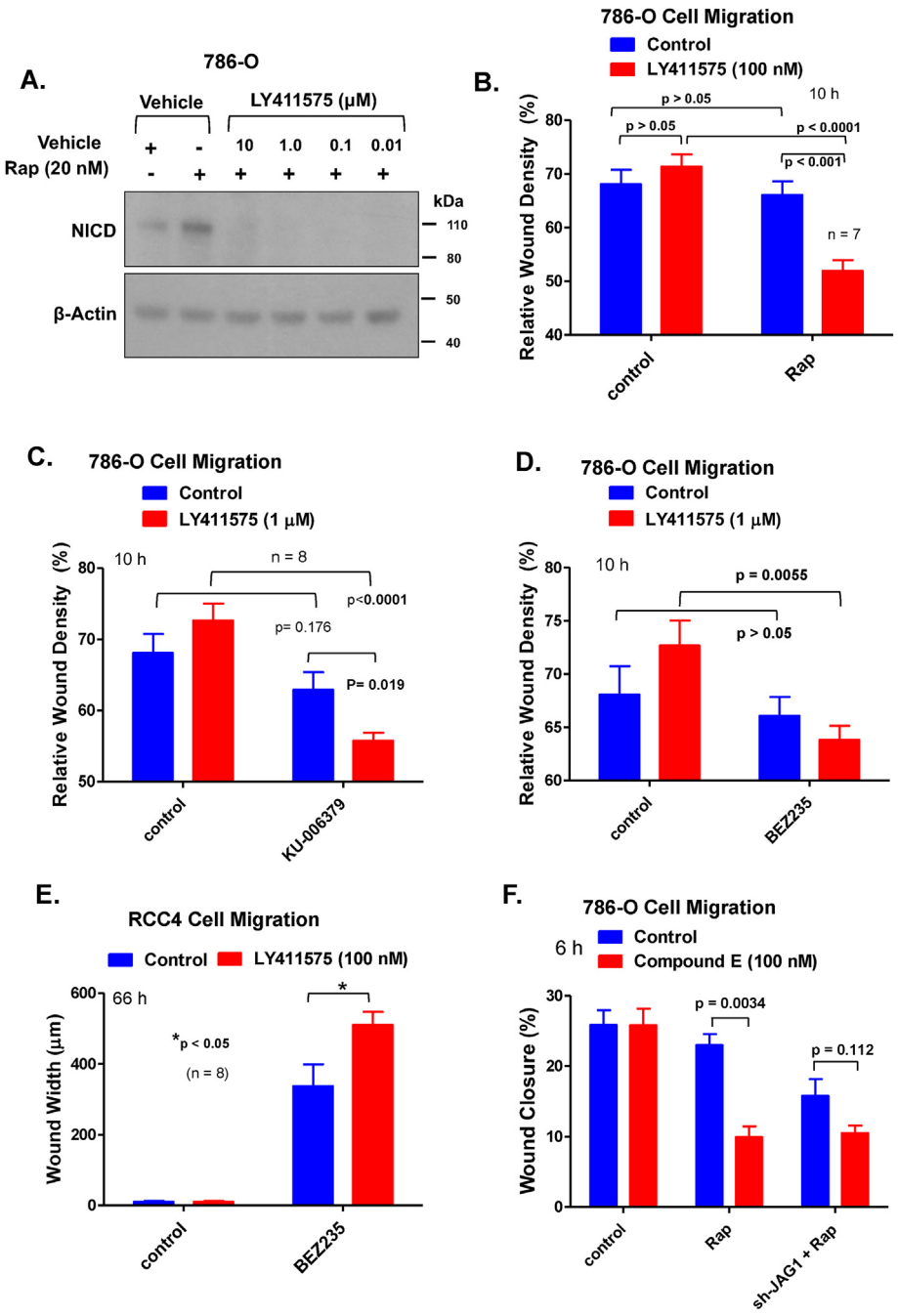

Fig. 9. Inhibition of Notch with γ-secretase inhibitors enhances the effectiveness of mTOR inhibitors in suppressing the migration of 786-O and RCC4 cells. A) Effect of various doses of LY411575 on suppressing the activation of Notch1 by 20 nM Rap (24 h treatment of 786-O cells) was assessed by Western blotting of Notch1 NICD. **B-E)** Effect of LY411575 on changes on the migration of 786–0 cells in response to 30 nM Rap **(B)**, 1 μM KU-0063794 **(C)**, and 100 nM BEZ235 **(D)** was assessed after 10 h of treatment by InCucyte Zoom live-cell imaging in InCucyte Imagelock 96-well plates. **E)** Effect of 100 nM LY411575 on the suppression of RCC4 cell migration by 100 nM BEZ235 was assessed by Wound Width after 66 h of treatment. **F)** Effect of Rap on the Wound Closure (%) of sh-scramble control versus JAG1-silenced 786-O cells (plated in 6-well dishes) was assessed 6 h after treatment with vehicle or 30 nM Rap either with or without 100 nM Compound E. Each point on the the above graphs is the average of 8 biological replicates ± SE. P-values were measured by two-way ANOVA using GraphPad Prism statistical tools.

et al., 2004) and is required for EMT induced by TGF-β1 in tubular renal epithelial cells (Zavadil et al., 2004).

The multiple potent oncogenic functions of TGF-β1, most significantly metastasis and evasion of tumor immune surveillance (Massague, 2008), have ignited an enormous effort to develop selective TGF-β inhibitors for clinical management of aggressive cancers, as thoroughly described elsewhere (Kim et al., 2021b). The findings of our study support that TGF-β antagonism may enhance the therapeutic efficacy of rapalogs as well as other mTOR inhibitors in the treatment of ccRCC by inhibiting JAG1 expression and Notch signaling. Recent findings supported that selective suppression of the TGF-β1 isoform, achieved by an antibody (named SRK-181) to the TGF-β1 latency-associated protein (LAP) that prevents the activation of TGF-β1, had robust anti-tumor suppressive activity without any cardiac or other overt toxicities associated with previous TGF-β antagonists. SRK-181 reversed immune checkpoint blockade and overcame resistance to anti-PD1 therapy in mice bearing syngeneic tumors (Martin et al., 2020).

In summary, our findings support that JAG1 is induced by the inhibition of mTOR in ccRCC through an Akt1/ALK5/Smad4-dependent mechanism, and this induction of JAG1 counteracts the effectiveness of mTOR inhibitors on those cancers. In particular, our data support that induced expression of JAG1 counteracts the action of mTOR inhibitors in suppressing ccRCC cell motility and spread. In the case of the RCC4 cell line, silencing JAG1 alone also robustly inhibited their growth. Based on our study and the literature, we propose that antagonizing the expression of JAG1 with an Akt1 kinase (e.g., MK2206), ALK5 or TGF-β1 inhibitor (e.g., SRK-181), or a γ-secretase inhibitor such as LY3039478 (Massard et al., 2018), may enhance the therapeutic efficacy of mTOR inhibitors in

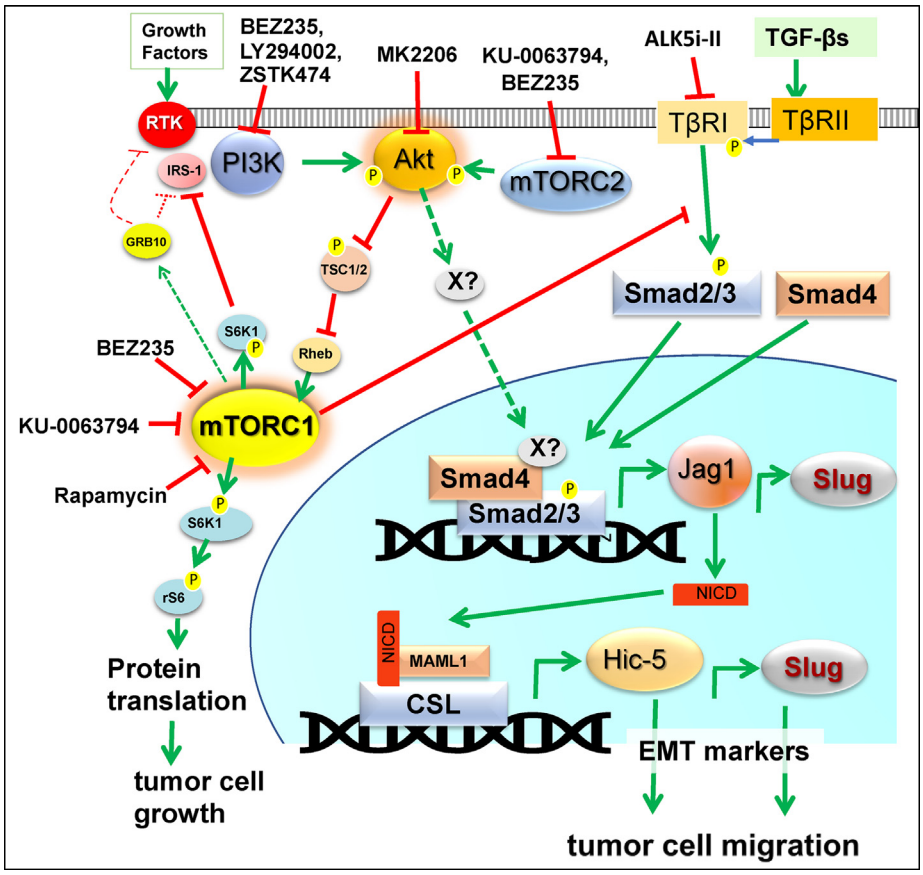

Fig. 10. A schematic representation of our proposed model explaining the potential mechanism by which mTOR inhibitors induce the expression of JAG1. Our data support that JAG1 is induced by mTOR inhibitors (Rap, KU-0063794, BEZ325) in RCC cells through a mechanism that is dependent on Akt and TGF-β/ALK5(TβRI)/Smad4 signaling. In this model, inhibition of mTORC1 activates Akt1 by directly relieving the inhibitory phosphorylation of IRS-1 or indirectly inhibiting IRS-1 by activating Grb10. mTOR inhibitors also activate TGF-β/Smad signaling by relieving mTOR's suppression of TβRI (ALK5). Both TGF-β1 and mTOR inhibitors induce the expression of Slug and Hic-5 through a mechanism that is additive/synergistic and at least partially dependent on the expression of JAG1. We hypothesize that a JAG1/Notch/TGF-β/Akt signaling network is activated in RCC cells by mTORC1 inhibitors and that such activation counteracts the effectiveness of mTOR inhibitor therapeutics.

VEGF-refractory ccRCC. A caveat with such combined therapeutic strategies is host toxicity. Thus, a more targeted approach of blocking JAG1 in ccRCC, such as a JAG1 neutralizing antibody already developed (Masiero et al., 2019), may prove to be a safer and more effective therapeutic strategy. Further work is necessary to test the *in vivo* significance of our findings and proposed model.

CRediT authorship contribution statement

David Danielpour: Conceptualization, Data curation, Formal analysis, Funding acquisition, Investigation, Methodology, Project administration, Resources, Supervision, Validation, Visualization, Writing – original draft, Writing – review & editing. **Sarah Corum:** Conceptualization, Data curation, Formal analysis. **Patrick Leahy:** Formal analysis, Writing – review & editing. **Anusha Bangalore:** Data curation.

Declaration of competing interest

The authors declare that the research was conducted in the absence of any financial interests/personal relationships which may be considered as potential competing interests.

Acknowledgments

This study was supported by the NIH grant R01CA134878, Bridge Funding Award BFA2014-004 from Case Western Reserve University (to D.D.), and the Case Comprehensive Cancer Center P30CA43703 for a GU malignancy pilot award and use of the gene expression core facility. The authors thank Martina Veigl, Chunbiao Li, and Debora Poruban for help with Affymetrix gene expression analysis. The Visual Abstract was created with BioRender.com.

Appendix A. Supplementary data

Supplementary data to this article can be found online at https://doi.org/10.1016/j.crphar.2022.100117.

References

Alzahrani, A.S., 2019. PI3K/Akt/mTOR inhibitors in cancer: at the bench and bedside. Semin. Cancer Biol. 59, 125–132.

Bao, J.M., Dang, Q., Lin, C.J., Lo, U.G., Feldkoren, B., Dang, A., Hernandez, E., Li, F., Panwar, V., Lee, C.F., Cen, J.J., Guan, B., Margulis, V., Kapur, P., Brekken, R.A., Luo, J.H., Hsieh, J.T., Tan, W.L., 2021. SPARC is a key mediator of TGF-beta-induced renal cancer metastasis. J. Cell. Physiol. 236 (3), 1926–1938.

Cancel, M., Fromont, G., Blonz, C., Chevreau, C., Rioux-Leclercq, N., Laguerre, B., Oudard, S., Gross-Goupil, M., Gravis, G., Goldwasser, F., Rolland, F., Delva, R., Moise, L., Emambux, S., Vassal, C., Zanetta, S., Penel, N., Flechon, A., Barthelemy, P., Saldana, C., Lefort, F., Escudier, B., Linassier, C., Albiges, L., 2021. Everolimus or sunitinib as first-line treatment of metastatic papillary renal cell carcinoma: a retrospective study of the GETUG group (Groupe d'Etude des Tumeurs Uro-Genitales). Eur. J. Cancer 158, 1–11.

Carlo, M.I., Molina, A.M., Lakhman, Y., Patil, S., Woo, K., DeLuca, J., Lee, C.H., Hsieh, J.J., Feldman, D.R., Motzer, R.J., Voss, M.H., 2016. A phase ib study of BEZ235, a dual inhibitor of phosphatidylinositol 3-kinase (PI3K) and mammalian target of rapamycin (mTOR), in patients with advanced renal cell carcinoma. Oncol. 21 (7), 787–788.

Carver, B.S., Chapinski, C., Wongvipat, J., Hieronymus, H., Chen, Y., Chandarlapaty, S., Arora, V.K., Le, C., Koutcher, J., Scher, H., Scardino, P.T., Rosen, N., Sawyers, C.L., 2011. Reciprocal feedback regulation of PI3K and androgen receptor signaling in PTEN-deficient prostate cancer. Cancer Cell 19 (5), 575–586.

Chauhan, A., Semwal, D.K., Mishra, S.P., Goyal, S., Marathe, R., Semwal, R.B., 2016. Combination of mTOR and MAPK inhibitors-A potential way to treat renal cell carcinoma. Med. Sci. 4 (4).

Chen, C.H., Hsia, T.C., Yeh, M.H., Chen, T.W., Chen, Y.J., Chen, J.T., Wei, Y.L., Tu, C.Y., Huang, W.C., 2017. MEK inhibitors induce Akt activation and drug resistance by suppressing negative feedback ERK-mediated HER2 phosphorylation at Thr701. Mol Oncol 11 (9), 1273–1287.

Chowdhury, N., Drake, C.G., 2020. Kidney cancer: an overview of current therapeutic approaches. Urol. Clin. 47 (4), 419–431.

Colland, F., Jacq, X., Trouplin, V., Mougin, C., Groizeleau, C., Hamburger, A., Meil, A., Wojcik, J., Legrain, P., Gauthier, J.M., 2004. Functional proteomics mapping of a human signaling pathway. Genome Res. 14 (7), 1324–1332.
Danielpour, D., Gao, Z., Zmina, P.M., Shankar, E., Shultes, B.C., Jobava, R., Welford, S.M., Hatzoglou, M., 2019. Early cellular responses of prostate carcinoma cells to sepantronium bromide (YM155) involve suppression of mTORC1 by AMPK. Sci. Rep. 9 (1), 11541.
Danielpour, D., Corum, S., Welford, S.M., Shankar, E., 2022. Hypoxia represses early responses of prostate and renal cancer cells to YM155 independent of HIF-1alpha and HIF-2alpha. Curr Res Pharmacol Drug Discov 3, 100076.
Downward, J., 1998. Mechanisms and consequences of activation of protein kinase B/Akt. Curr. Opin. Cell Biol. 10 (2), 262–267.
Drenan, R.M., Liu, X., Bertram, P.G., Zheng, X.F., 2004. FKBP12-rapamycin-associated protein or mammalian target of rapamycin (FRAP/mTOR) localization in the endoplasmic reticulum and the Golgi apparatus. J. Biol. Chem. 279 (1), 772–778.
Easton, J.B., Kurmasheva, R.T., Houghton, P.J., 2006. IRS-1: auditing the effectiveness of mTOR inhibitors. Cancer Cell 9 (3), 153–155.
Flaherty, K.T., Manola, J.B., Pins, M., McDermott, D.F., Atkins, M.B., Dutcher, J.J., George, D.J., Margolin, K.A., DiPaola, R.S., 2015. BEST: a randomized phase II study of vascular endothelial growth factor, RAF kinase, and mammalian target of rapamycin combination targeted therapy with bevacizumab, sorafenib, and temsirolimus in advanced renal cell carcinoma–A trial of the ECOG-ACRIN cancer research group (E2804). J. Clin. Oncol. 33 (21), 2384–2391.
Garcia, J.A., Danielpour, D., 2008. Mammalian target of rapamycin inhibition as a therapeutic strategy in the management of urologic malignancies. Mol. Cancer Therapeut. 7 (6), 1347–1354.
Garcia-Martinez, J.M., Moran, J., Clarke, R.G., Gray, A., Cosulich, S.C., Chresta, C.M., Alessi, D.R., 2009. Ku-0063794 is a specific inhibitor of the mammalian target of rapamycin (mTOR). Biochem. J. 421 (1), 29–42.
Gellibert, F., Woolven, J., Fouchet, M.H., Mathews, N., Goodland, H., Lovegrove, V., Laroze, A., Nguyen, V.L., Sautet, S., Wang, R., Janson, C., Smith, W., Krysa, G., Boullay, V., De Gouville, A.C., Huet, S., Hartley, D., 2004. Identification of 1,5-naphthyridine derivatives as a novel series of potent and selective TGF-beta type I receptor inhibitors. J. Med. Chem. 47 (18), 4494–4506.
Gupta, S., Hau, A.M., Beach, J.R., Harwalker, J., Mantuano, E., Gonias, S.L., Egelhoff, T.T., Hansel, D.E., 2013. Mammalian target of rapamycin complex 2 (mTORC2) is a critical determinant of bladder cancer invasion. PLoS One 8 (11), e81081.
Hao, Y., Baker, D., Ten Dijke, P., 2019. TGF-beta-Mediated epithelial-mesenchymal transition and cancer metastasis. Int. J. Mol. Sci. 20 (11).
Hess, G., Herbrecht, R., Romaguera, J., Verhoef, G., Crump, M., Gisselbrecht, C., Laurell, A., Offner, F., Strahs, A., Berkenblit, A., Hanushevsky, O., Clancy, J., Hewes, B., Moore, L., Coiffier, B., 2009. Phase III study to evaluate temsirolimus compared with investigator's choice therapy for the treatment of relapsed or refractory mantle cell lymphoma. J. Clin. Oncol. 27 (23), 3822–3829.
Hsu, P.P., Kang, S.A., Rameseder, J., Zhang, Y., Ottina, K.A., Lim, D., Peterson, T.R., Choi, Y., Gray, N.S., Yaffe, M.B., Marto, J.A., Sabatini, D.M., 2011. The mTOR-regulated phosphoproteome reveals a mechanism of mTORC1-mediated inhibition of growth factor signaling. Science 332 (6035), 1317–1322.
Inoki, K., Li, Y., Xu, T., Guan, K.L., 2003. Rheb GTPase is a direct target of TSC2 GAP activity and regulates mTOR signaling. Genes Dev. 17 (15), 1829–1834.
Jacob, A., Shook, J., Hutson, T., 2021. The implementation of lenvatinib/everolimus or lenvatinib/pembrolizumab combinations in the treatment of metastatic renal cell carcinoma. Expert Rev. Anticancer Ther. 21 (4), 365–372.
Jia, S., Meng, A., 2021. TGFbeta family signaling and development. Development 148 (5).
Kalra, S., Atkinson, B.J., Matrana, M.R., Matin, S.F., Wood, C.G., Karam, J.A., Tamboli, P., Sircar, K., Rao, P., Corn, P.G., Tannir, N.M., Jonasch, E., 2016. Prognosis of patients with metastatic renal cell carcinoma and pancreatic metastases. BJU Int. 117 (5), 761–765.
Kerr, B.A., West, X.Z., Kim, Y.W., Zhao, Y., Tischenko, M., Cull, R.M., Phares, T.W., Peng, X.D., Bernier-Latmani, J., Petrova, T.V., Adams, R.H., Hay, N., Naga Prasad, S.V., Byzova, T.V., 2016. Stability and function of adult vasculature is sustained by Akt/Jagged1 signalling axis in endothelium. Nat. Commun. 7, 10960.
Kim, D.H., Sarbassov, D.D., Ali, S.M., King, J.E., Latek, R.R., Erdjument-Bromage, H., Tempst, P., Sabatini, D.M., 2002. mTOR interacts with raptor to form a nutrient-sensitive complex that signals to the cell growth machinery. Cell 110 (2), 163–175.
Kim, J., Kundu, M., Viollet, B., Guan, K.L., 2011. AMPK and mTOR regulate autophagy through direct phosphorylation of Ulk1. Nat. Cell Biol. 13 (2), 132–141.
Kim, H., Shim, B.Y., Lee, S.J., Lee, J.Y., Lee, H.J., Kim, I.H., 2021a. Loss of Von Hippel-Lindau (VHL) tumor suppressor gene function: VHL-HIF pathway and advances in treatments for metastatic renal cell carcinoma (RCC). Int. J. Mol. Sci. 22 (18).
Kim, B.G., Malek, E., Choi, S.H., Ignatz-Hoover, J.J., Driscoll, J.J., 2021b. Novel therapies emerging in oncology to target the TGF-beta pathway. J. Hematol. Oncol. 14 (1), 55.
Kohn, A.D., Takeuchi, F., Roth, R.A., 1996. Akt, a pleckstrin homology domain containing kinase, is activated primarily by phosphorylation. J. Biol. Chem. 271 (36), 21920–21926.
Kominsky, S.L., Doucet, M., Brady, K., Weber, K.L., 2007. TGF-beta promotes the establishment of renal cell carcinoma bone metastasis. J. Bone Miner. Res. 22 (1), 37–44.
Kushida, N., Nomura, S., Mimura, I., Fujita, T., Yamamoto, S., Nangaku, M., Aburatani, H., 2016. Hypoxia-inducible factor-1alpha activates the transforming growth factor-beta/SMAD3 pathway in kidney tubular epithelial cells. Am. J. Nephrol. 44 (4), 276–285.
Maira, S.M., Stauffer, F., Brueggen, J., Furet, P., Schnell, C., Fritsch, C., Brachmann, S., Chene, P., De Pover, A., Schoemaker, K., Fabbro, D., Gabriel, D., Simonen, M., Murphy, L., Finan, P., Sellers, W., Garcia-Echeverria, C., 2008. Identification and characterization of NVP-BEZ235, a new orally available dual phosphatidylinositol 3-kinase/mammalian target of rapamycin inhibitor with potent in vivo antitumor activity. Mol. Cancer Therapeut. 7 (7), 1851–1863.
Mallikarjuna, P., Raviprakash, T.S., Aripaka, K., Ljungberg, B., Landstrom, M., 2019. Interactions between TGF-beta type I receptor and hypoxia-inducible factor-alpha mediates a synergistic crosstalk leading to poor prognosis for patients with clear cell renal cell carcinoma. Cell Cycle 18 (17), 2141–2156.
Martin, C.J., Datta, A., Littlefield, C., Kalra, A., Chapron, C., Wawersik, S., Dagbay, K.B., Brueckner, C.T., Nikiforov, A., Danehy Jr., F.T., Streich Jr., F.C., Boston, C., Simpson, A., Jackson, J.W., Lin, S., Danek, N., Faucette, R.R., Raman, P., Capili, A.D., Buckler, A., Carven, G.J., Schurpf, T., 2020. Selective inhibition of TGFbeta1 activation overcomes primary resistance to checkpoint blockade therapy by altering tumor immune landscape. Sci. Transl. Med. 12 (536).
Maru, S., Ishigaki, Y., Shinohara, N., Takata, T., Tomosugi, N., Nonomura, K., 2013. Inhibition of mTORC2 but not mTORC1 up-regulates E-cadherin expression and inhibits cell motility by blocking HIF-2alpha expression in human renal cell carcinoma. J. Urol. 189 (5), 1921–1929.
Masiero, M., Li, D., Whiteman, P., Bentley, C., Greig, J., Hassanali, T., Watts, S., Stribbling, S., Yates, J., Bealing, E., Li, J.L., Chillakuri, C., Sheppard, D., Serres, S., Sarmiento-Soto, M., Larkin, J., Sibson, N.R., Handford, P.A., Harris, A.L., Banham, A.H., 2019. Development of therapeutic anti-JAGGED1 antibodies for cancer therapy. Mol. Cancer Therapeut. 18 (11), 2030–2042.
Massague, J., 1998. TGF-beta signal transduction. Annu. Rev. Biochem. 67, 753–791.
Massague, J., 2008. TGFbeta in cancer. Cell 134 (2), 215–230.
Massard, C., Azaro, A., Soria, J.C., Lassen, U., Le Tourneau, C., Sarker, D., Smith, C., Ohnmacht, U., Oakley, G., Patel, B.K.R., Yuen, E.S.M., Benhadji, K.A., Rodon, J., 2018. First-in-human study of LY3039478, an oral Notch signaling inhibitor in advanced or metastatic cancer. Ann. Oncol. 29 (9), 1911–1917.
Morikawa, M., Derynck, R., Miyazono, K., 2016. TGF-Beta and the TGF-beta family: context-dependent roles in cell and tissue physiology. Cold Spring Harbor Perspect. Biol. 8 (5).
Moses, H.L., Roberts, A.B., Derynck, R., 2016. The discovery and early days of TGF-beta: a historical perspective. Cold Spring Harbor Perspect. Biol. 8 (7).
Naber, H.P., Drabsch, Y., Snaar-Jagalska, B.E., ten Dijke, P., van Laar, T., 2013. Snail and Slug, key regulators of TGF-beta-induced EMT, are sufficient for the induction of single-cell invasion. Biochem. Biophys. Res. Commun. 435 (1), 58–63.
Noseda, M., McLean, G., Niessen, K., Chang, L., Pollet, I., Montpetit, R., Shahidi, R., Dorovini-Zis, K., Li, L., Beckstead, B., Durand, R.E., Hoodless, P.A., Karsan, A., 2004. Notch activation results in phenotypic and functional changes consistent with endothelial-to-mesenchymal transformation. Circ. Res. 94 (7), 910–917.
Nyhan, K.C., Faherty, N., Murray, G., Cooey, L.B., Godson, C., Crean, J.K., Brazil, D.P., 2010. Jagged/Notch signalling is required for a subset of TGFbeta1 responses in human kidney epithelial cells. Biochim. Biophys. Acta 1803 (12), 1386–1395.
Oon, C.E., Bridges, E., Sheldon, H., Sainson, R.C.A., Jubb, A., Turley, H., Leek, R., Buffa, F., Harris, A.L., Li, J.L., 2017. Role of Delta-like 4 in Jagged1-induced tumour angiogenesis and tumour growth. Oncotarget 8 (25), 40115–40131.
Pandey, J., Syed, W., 2021. Renal cancer. In: StatPearls. Treasure Island (FL).
Pezzicoli, G., Filoni, E., Gernone, A., Cosmai, L., Rizzo, M., Porta, C., 2021. Playing the devil's advocate: should we give a second chance to mTOR inhibition in renal clear cell carcinoma? - ie strategies to revert resistance to mTOR inhibitors. Cancer Manag. Res. 13, 7623–7636.
Pignatelli, J., Tumbarello, D.A., Schmidt, R.P., Turner, C.E., 2012. Hic-5 promotes invadopodia formation and invasion during TGF-beta-induced epithelial-mesenchymal transition. J. Cell Biol. 197 (3), 421–437.
Sarbassov, D.D., Ali, S.M., Kim, D.H., Guertin, D.A., Latek, R.R., Erdjument-Bromage, H., Tempst, P., Sabatini, D.M., 2004. Rictor, a novel binding partner of mTOR, defines a rapamycin-insensitive and raptor-independent pathway that regulates the cytoskeleton. Curr. Biol. 14 (14), 1296–1302.
Sarbassov, D.D., Ali, S.M., Sengupta, S., Sheen, J.H., Hsu, P.P., Bagley, A.F., Markhard, A.L., Sabatini, D.M., 2006. Prolonged rapamycin treatment inhibits mTORC2 assembly and Akt/PKB. Mol. Cell. 22 (2), 159–168.
Saxton, R.A., Sabatini, D.M., 2017. mTOR signaling in growth, metabolism, and disease. Cell 168 (6), 960–976.
Shen, Wei, Huang, Jiaxin, Wang, Yan, 2021. Biological significance of NOTCH signaling strength. Front. Cell Dev. Biol. 9, 652273. https://doi.org/10.3389/fcell.2021.652273.
Shi, Y., Yan, H., Frost, P., Gera, J., Lichtenstein, A., 2005. Mammalian target of rapamycin inhibitors activate the AKT kinase in multiple myeloma cells by up-regulating the insulin-like growth factor receptor/insulin receptor substrate-1/phosphatidylinositol 3-kinase cascade. Mol. Cancer Therapeut. 4 (10), 1533–1540.
Sitaram, R.T., Mallikarjuna, P., Landstrom, M., Ljungberg, B., 2016. Transforming growth factor-beta promotes aggressiveness and invasion of clear cell renal cell carcinoma. Oncotarget 7 (24), 35917–35931.
Sjolund, J., Johansson, M., Manna, S., Norin, C., Pietras, A., Beckman, S., Nilsson, E., Ljungberg, B., Axelson, H., 2008. Suppression of renal cell carcinoma growth by inhibition of Notch signaling in vitro and in vivo. J. Clin. Invest. 118 (1), 217–228.
Sjolund, J., Bostrom, A.K., Lindgren, D., Manna, S., Moustakas, A., Ljungberg, B., Johansson, M., Fredlund, E., Axelson, H., 2011. The notch and TGF-beta signaling pathways contribute to the aggressiveness of clear cell renal cell carcinoma. PLoS One 6 (8), e23057.
Smith, S.F., Collins, S.E., Charest, P.G., 2020. Ras, PI3K and mTORC2 - three's a crowd? J. Cell Sci. 133 (19).
Song, K., Wang, H., Krebs, T.L., Danielpour, D., 2006. Novel roles of Akt and mTOR in suppressing TGF-beta/ALK5-mediated Smad3 activation. EMBO J. 25 (1), 58–69.
Song, K., Shankar, E., Yang, J., Bane, K.L., Wahdan-Alaswad, R., Danielpour, D., 2013. Critical role of a survivin/TGF-beta/mTORC1 axis in IGF-I-mediated growth of prostate epithelial cells. PLoS One 8 (5), e61896.

Staehler, M., Stockle, M., Christoph, D.C., Stenzl, A., Potthoff, K., Grimm, M.O., Klein, D., Harde, J., Bruning, F., Goebell, P.J., Augustin, M., Roos, F., Benz-Rud, I., Marschner, N., Grunwald, V., 2021. Everolimus after failure of one prior VEGF-targeted therapy in metastatic renal cell carcinoma: final results of the MARC-2 trial. Int. J. Cancer 148 (7), 1685–1694.

Sun, S.Y., 2021. mTOR-targeted cancer therapy: great target but disappointing clinical outcomes, why? Front. Med. 15 (2), 221–231.

Taylor, C., Craven, R.A., Harnden, P., Selby, P.J., Banks, R.E., 2012. Determination of the consequences of VHL mutations on VHL transcripts in renal cell carcinoma. Int. J. Oncol. 41 (4), 1229–1240.

Tirpe, A.A., Gulei, D., Ciortea, S.M., Crivii, C., Berindan-Neagoe, I., 2019. Hypoxia: overview on hypoxia-mediated mechanisms with a focus on the role of HIF genes. Int. J. Mol. Sci. 20 (24).

Tremblay, F., Marette, A., 2001. Amino acid and insulin signaling via the mTOR/p70 S6 kinase pathway. A negative feedback mechanism leading to insulin resistance in skeletal muscle cells. J. Biol. Chem. 276 (41), 38052–38060.

Tumbarello, D.A., Turner, C.E., 2007. Hic-5 contributes to epithelial-mesenchymal transformation through a RhoA/ROCK-dependent pathway. J. Cell. Physiol. 211 (3), 736–747.

Wang, Z., Li, Y., Kong, D., Banerjee, S., Ahmad, A., Azmi, A.S., Ali, S., Abbruzzese, J.L., Gallick, G.E., Sarkar, F.H., 2009. Acquisition of epithelial-mesenchymal transition phenotype of gemcitabine-resistant pancreatic cancer cells is linked with activation of the notch signaling pathway. Cancer Res. 69 (6), 2400–2407.

Wang, W., Wang, L., Mizokami, A., Shi, J., Zou, C., Dai, J., Keller, E.T., Lu, Y., Zhang, J., 2017. Down-regulation of E-cadherin enhances prostate cancer chemoresistance via Notch signaling. Chin. J. Cancer 36 (1), 35.

Wirsik, N.M., Ehlers, J., Mader, L., Ilina, E.I., Blank, A.E., Grote, A., Feuerhake, F., Baumgarten, P., Devraj, K., Harter, P.N., Mittelbronn, M., Naumann, U., 2021. TGF-beta activates pericytes via induction of the epithelial-to-mesenchymal transition protein SLUG in glioblastoma. Neuropathol. Appl. Neurobiol. 47 (6), 768–780.

Wu, K., Xu, L., Zhang, L., Lin, Z., Hou, J., 2011. High Jagged1 expression predicts poor outcome in clear cell renal cell carcinoma. Jpn. J. Clin. Oncol. 41 (3), 411–416.

Wu, K., Hu, L., Hou, J., 2016. Selective suppression of Notch1 inhibits proliferation of renal cell carcinoma cells through JNK/p38 pathway. Oncol. Rep. 35 (5), 2795–2800.

Yang, S.D., Sun, R.C., Mu, H.J., Xu, Z.Q., Zhou, Z.Y., 2010. The expression and clinical significance of TGF-beta1 and MMP2 in human renal clear cell carcinoma. Int. J. Surg. Pathol. 18 (2), 85–93.

Zavadil, J., Cermak, L., Soto-Nieves, N., Bottinger, E.P., 2004. Integration of TGF-beta/Smad and Jagged1/Notch signalling in epithelial-to-mesenchymal transition. EMBO J. 23 (5), 1155–1165.

Zhang, J., Gao, Z., Yin, J., Quon, M.J., Ye, J., 2008. S6K directly phosphorylates IRS-1 on Ser-270 to promote insulin resistance in response to TNF-(alpha) signaling through IKK2. J. Biol. Chem. 283 (51), 35375–35382.

Zhou, S., Buckhaults, P., Zawel, L., Bunz, F., Riggins, G., Dai, J.L., Kern, S.E., Kinzler, K.W., Vogelstein, B., 1998. Targeted deletion of Smad4 shows it is required for transforming growth factor beta and activin signaling in colorectal cancer cells. Proc. Natl. Acad. Sci. U. S. A. 95 (5), 2412–2416.